EFFECTS OF QUENCHING AND ANNEALING ON IONIC CONDUCTIVITY IN LITHIUM FLUORIDE

Jong Keel Lee

Washington University

1969

EFFECTS OF QUENCHING AND ANNEALING ON IONIC CONDUCTIVITY IN LITHIUM FLUORIDE

BY

JONG KEEL LEE

A thesis submitted in partial fulfillment

of the requirements for the degree of

MASTER OF SCIENCE

IN

METALLURGICAL ENGINEERING

UNIVERSITY OF WASHINTON

1969

Approved by Thomas G. Stoebe

Department Mining, Metallurgical & Ceramic Engr.

Date May 28, 1969

In presenting this thesis in partial fulfillment of the requirements of an advanced degree at the University of Washington I agree that the Library shall make it freely available for inspection. I further agree that permission for extensive copying of this thesis for scholarly purposes may be granted by my major professor, or, in his absence, by the Director of Libraries. It is understood that any copying or publication of this thesis for financial gain shall not be allowed without my written permission.

Signature Tony K. Lee

Date May 25 1963

ABSTRACT

Ionic conductivity measurements of pure and Mg-doped LiF crystals have been made in the temperature range room temperature to 600°C. The whole conductivity plot was divided into seven regions. In the high temperature part of intrinsic region, the anion-vacancy contribution to the ionic conductivity was confirmed. The formation energy of a Schottky pair is 2.30 eV, while the activation energy for cation vacancy motion is 0.72 $\pm$ 0.02 eV.

From the annealing-out of the excess conductivity in quenched LiF crystals, it is found that the decay behavior of excess quenched-in vacancies in LiF crystals follows first-order kinetics. When quenching strains occur, there exists an anomalous increase in conductivity during annealing. This anomalous increase is probably due to the release of free cation vacancies which are bound to dislocations during quenching.

ACKNOWLEDGEMENTS

The author wishes to express his sincere thanks and gratitude to Dr. T. G. Stoebe, Associate Professor of Metallurgical Engineering, for advice and encouragements during all the phases of this work. He is especially grateful to him for a number of enlightening discussions. He also wishes to thank Dr. H. I. Dawson for helpful discussions and continuous encouragement and Mr. R. L. Trantow for his work on the ionic conduction instrumentation. He would like to thank his wife, Sangja, for her assistance.

This work was supported by the Graduate School Research Fund at the University of Washington, the National Science Foundation, the NASA Ceramic Materials Research Grant (NGL-48-002-004), and the Institutional Research Grant from the American Cancer Society.

TABLE OF CONTENTS

(Cont.)

LIST OF FIGURES

(cont.)

LIST OF TABLES

INTRODUCTION

The alkali halides have been a classical subject for the investigation of defects in crystals. Their usefulness in the study of defects is connected with the comparatively direct information obtainable from electrical measurements, particularly the ionic conductivity.

A summary of the many investigations dealing with the ionic conductivity has been given by Lidiard (1), and recently by Suptitz and Teltow (2). Since the early work of Lehfeldt (3) and Koch and Wagner (4), many conclusions have been drawn from ionic conductivity experiments. Dreyfus and Nowick (5), and Kirk and Pratt (6) have carried out thorough investigations on ionic conductivity of sodium chloride at low temperature as well as at high temperature.

The early work of Haven (7) (8) on Mg-doped LiF showed that the formation energy of a Shottky pair was 2.68eV and the motion energy of a cation vacancy was 0.72eV, which was taken by replotting as σT (9). Stoebe and Pratt (9) made conductivity measurements on LiF, and showed the motion energy of a cation vacancy to be 0.70 ± 0.02eV and the formation energy of a Schottky pair to be 2.34eV, using NMR diffusion data. Barsis et. al (10) reported 0.73eV as the motion energy of a cation

vacancy and 2.4eV as the formation energy of a Schottky pair. Although there have been many investigations on LiF, their values on energy term such as activation energy for motion of cation vacancy have always shown small differencies in magnitude. Also few experiments have been done in the low temperature region. Therefore, a study of the ionic conductivity over a wide temperature range was undertaken for better information of ionic conductivity of LiF.

In order to investigate the state of defects as well as interactions among them, quenching and annealing experiments seemed desirable. However, the small thermal conductivity of ionic crystals, and the difficulty of avoiding quenching strains at high quenching rates have not allowed many successful experiments, and thus very little work has been performed on the quenching and annealing behavior of ionic crystals (5) (16) (15). Moreover, most of the previous work used quenching rates which did not exceed 50°C/min. Thus a further object of this work is to study the annealing behavior of quenched specimens, using high quenching rates (500 - 600°C/min), both on thin specimens and on thick specimens of LiF.

T H E O R Y

A) Ionic Conductivity in Alkali Halides

The ionic conductivity of alkali halide crystals of the NaCl type occurs predominantly through the motion of vacancies (1). Further investigations (11)(12) have established that, except near the melting point, the electric current is carried almost entirely by the motion of cations. Accordingly, the cation vacancy is regarded as the mobile charge carrier. The electrical conductivity, σ, is then given by the following expression :

$$\sigma = [V] Ne\mu = [V] N\left(\frac{e^2 a^2 \nu_0}{kT}\right) \exp(-E_m/kT) \quad . \quad . \quad . \quad (1)$$

where $[V]$ is the mole fraction of cation vacancies, μ is the mobility of the vacancy, N is the number of cation lattice sites per unit volume, a is the lattice parameter, E_m is the activation energy for motion of a cation vacancy, ν_0 is a frequency factor, which also contains an entropy factor and e and kT have their usual meanings.

From equation (1) it follows that a plot of log σT vs. 1/T should yield a straight line. The slope of this line represents an effective activation energy which is equal to E_m plus an energy associated with the temperature dependence of $[V]$. A schematic diagram of the

conductivity plot, showing the regions which have been definitely established, is presented in figure 1. In region I, which is known as the intrinsic region, $[V]$ is the equilibrium concentration of Schottky defects in the lattice, given by

$$[V] = \exp(S_S/2k - E_S/2kT) \qquad \ldots (2)$$

where S_S and E_S are the entropy and energy of formation of a Schottky defect.

Combining equations (1) and (2) shows that the conductivity is governed by a relation of the type

$$\sigma T = (\text{const.}) \exp\left[-(\tfrac{1}{2}E_S + E_m)/kT\right] \qquad \ldots (3)$$

and thus the effective activation energy, E_I, for region I is given by

$$E_I = E_m + \tfrac{1}{2}E_S \qquad \ldots (4)$$

At lower temperatures, the cation vacancies have a different origin. These are the vacancies which accompany divalent metallic impurity ions so as to maintain the overall charge neutrality of the crystal. When the number of vacancies introduced by divalent cation impurities exceeds the number produced thermally, the conductivity yields to region II. In this region, the

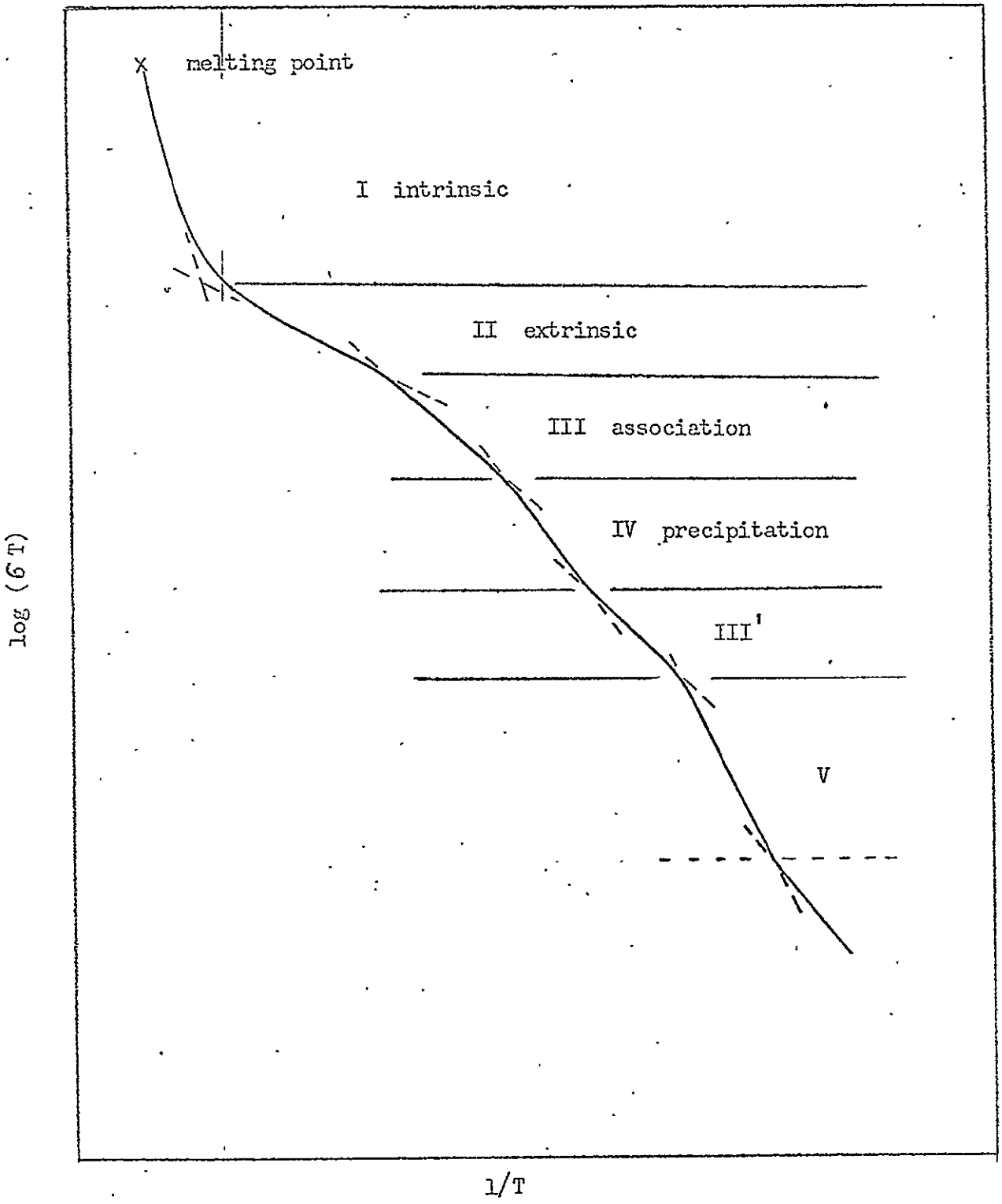

Figure 1. A schematic ionic conductivity-temperature plot for NaCl-type ionic crystals.

mole fraction of cation vacancies is a constant, equal to the total mole fraction of divalent metallic impurities, $[M]$: from equation (1) therefore the effective activation energy, E_{II}, for this region is simply equal to E_m. Thus :

$$[V] = [M] = \text{const.}$$
$$E_{II} = E_m \qquad \ldots (5)$$

Based on the above considerations, one could hope to determine E_s and E_m separately from a knowledge of E_I and E_{II}. The difficulty in obtaining such values has been in part due to the fact that region II extends over only a limited conductivity range (9) and also due to the possibility that Debye-Huckel type interactions modify the interpretation (1)(5).

Two reasons have been given for the failure of region II to continue to low temperatures. The first one is the tendency of the oppositely charged divalent ion and the cation vacancy to associate to form a neutral complex. The second one is the precipitation of divalent impurity ions at temperatures where their concentration in solution begins to exceed the solubility limit. Both of these effects result in a decrease in $[V]$ below the value of $[M]$, and therefore can account for the end of region II, as shown in figure 1.

The effect of the association reaction on the conductivity is easily calculated for dilute solutions. The reaction itself may be expressed in the form

$$M\,V \rightleftharpoons M + V \qquad \ldots (6)$$

where M and V represent the divalent impurity ion and the cation vacancy respectively, and MV, the association complex. Application of elementary statistical mechanics to this reaction gives

$$\frac{[Mi]\cdot[V]}{[MV]} = K = \frac{1}{\sum_j Z_j \exp(E_j/kT)} \qquad \ldots (7)$$

where $[MV]$ is the mole fraction of the MV complex, $[Mi]$ is the mole fraction of isolated impurity ions. The subscript j refers to the various bound states in which the pair may be found, and Z_j and E_j are the number of possible configurations and the binding energy, respectively, for state j. In most cases the values of E_j for one or two of the closest bound states is distinctly larger than that for the higher states, so that the summation is reasonably replaced by a single term, $Z_A \exp(E_A/kT)$. The following auxilliary relations are added to equation (7) :

$$[V] = [Mi] \qquad \ldots (8)$$

$$[Mi] + [MV] = [M] \qquad \ldots (9)$$

The first of these expresses the condition of charge neutrality, while the second expresses the conservation of the impurities. Equations (7), (8) and (9) may then be solved for $[V]$. Of particular interest is the solution at the lower temperatures, where association is almost complete (i.e., $[V] \ll [M]$). The result obtained is

$$[V] = (\text{const.}) \exp(-E_A/2kT) \qquad \ldots (10)$$

If region III is due to this association reaction, then combining equation (10) with equation (1) gives for the effective energy,

$$E_{III} = E_m + \tfrac{1}{2}E_A \qquad \ldots (11)$$

However this is doubtful because this procedure assumes that all the impurities are in solution and that the conductivity plot in the association region is linear (6). In most cases this region is curved, a linear region appearing only in the most highly doped crystals.

As the temperature decreases further, the impurities in solution segregate or precipitate out from the solid solution. This results in a steepening of the conductivity plot giving region IV, the precipitation region. When this precipitation region is complete, the association between impurity and vacancy is said to continue (6), (13), (14).

After this region, the precipitation of a stable phase or a metastable phase again would follow but in these lower temperature regions, the conductivity is strongly dependent on the previous heat treatment as well as the amount of divalent impurities (10). Several regions occur below 150°C, but the mechanism for this formation is unclear.

B) Effect of Quenching on the Conductivity of Alkali Halides

The possibility of quenched-in defects is based on the fact that a finite time is required for the defects to establish themselves in equilibrium configurations. Thus when the crystal is being cooled the lattice defects will disappear continually. They disappear by the migration of the vacancies to the crystal surface, to grain boundaries, and to jog sites on dislocations. As the crystal is cooled and the defects become rapidly less mobile, the time required to establish equilibrium becomes correspondingly longer so that there comes a point at which the concentration of defects becomes effectively independent of temperature. In this state, the time to establish equilibrium is longer than the time required to measure the conductivity. Theoretically, if the quenching rate from temperature T_q is infinitely large and the temperature

to which the quench is made sufficiently low, we can expect to freeze in the vacancy concentration determined by equation (2). Experimentally, a finite fraction of vacancies are always lost during the quench.

A great number of experiments have been performed in metals to quench-in a measureable number of vacancies by rapid cooling of very thin wires. In the case of ionic crystals, the poor thermal conductivity makes it almost impossible to avoid large temperature gradients and large quenching stresses brought about by the differential thermal contraction. These can be large enough to lead to plastic deformation of the crystal and thus to a large conductivity increase due to the increase in the amount of vacancies.

In fact, only a few quenching experiments have been done, presumably because of this difficulty (5), (15), (16), (23). Quenching rates so far used in ionic crystals are slower than $100^{o}C/min$, whereas in the case of metals the rate exceeds 10^{4} $^{o}C/sec$. Table 1 shows quenching methods and quenching rates that were used in recent experiments.

One can expect that the fastest quench is most desirable because it achieves the greatest retention and the least association of vacancies and clusters during the

Table 1

Quenching methods and quenching rates

authors	quenching method	quenching rate	materials
Dreyfus and Nowick (5)	N_2 gas flow	20-50°C/min	NaCl
Layer et. al (15)	air quench	$<$ 10°C/min	AgCl
Ninomiya (16)	"	$<$ 10°C/min	KCl
Quin et. al (17)	"	15°C/hr	NaCl
Cook and Dryden (18)	"	$<$ 10°C/min	NaCl

quench. However, a quench always produces some thermal stresses since the interior and exterior parts of any specimen cool at different rates. If the thermal stresses become sufficiently large to cause plastic deformation, moving dislocations will be generated in the specimen. During dislocation motion, defects are generated in a nonthermodynamic way, and the equilibrium treatment may be seriously in error.

Avoiding these complications is highly desirable and can be accomplished by limiting the quenching rate to a value below which no plastic deformation occurs. Johnston (19) carried out quench-hardening experiments on lithium fluoride with a quenching temperature of 400°C, and various quenching rates. As shown in figure 2, in pure crystals, the flow stress is independent of the quenching rate if it is below $\sim$100°C/min, whereas in case of the impure crystal, the flow stress is decreasing until the quenching rate reaches $\sim$100°C/min. The decrease of flow stress in the impure crystal seems to be due to precipitates of impurities at slow quenching rates. According to this result, one can take the highest quenching rate $\sim$100°C/min with a specimen size of 10 x 2.5 x 2.5mm.

If impurities are present one should realize that

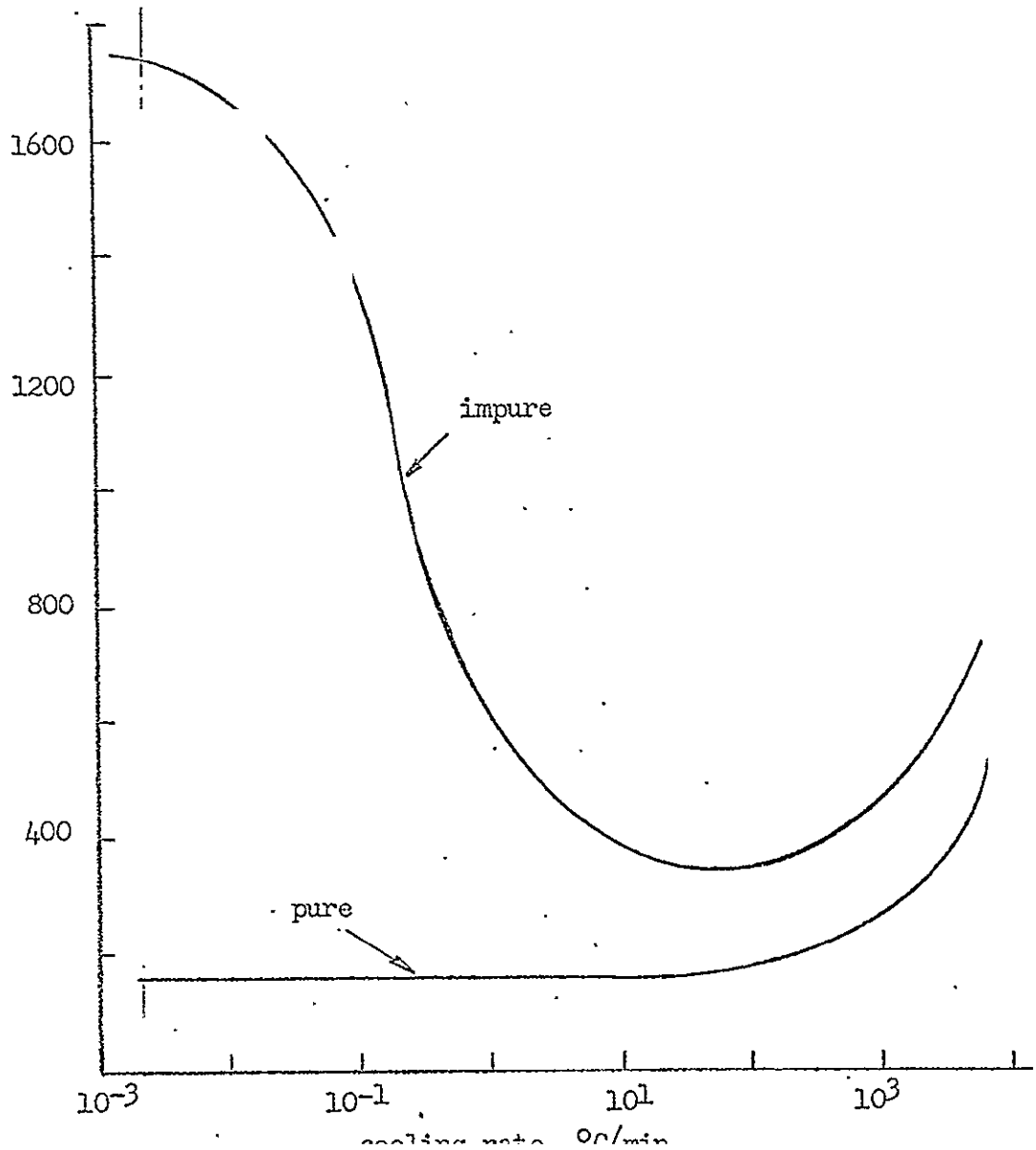

Figure 2. Effect of cooling rate from 400°C on the room temperature critical resolved shear stress of relatively pure and impure LiF single crystals.(19)

various complications could occur. A quench from the extrinsic region would change the relative distribution of free vacancies, dipoles, and larger aggregates. Quenching from the intrinsic region of an impure crystal may also produce dipoles in addition to extra vacancies.

C) Annealing After Quenching

In a quenched crystal, there exists a thermodynamic driving force to reduce the concentration of the defects to the equilibrium concentration characteristic of the crystal temperature. Annealing is the process of disappearance of a defect from a supersaturated crystal. Whether a sufficient number of defects disappear at any given temperature in a reasonable length of time depends upon their mobility. It has been known that the mobility of point defects increase rapidly with increasing temperature (5), and that a suitable temperature interval can always be found in which the disappearance of a given defect can be observed. However, the disappearance of a point defect cluster, or associate may not be controlled by the migration energy of the point defect but may arise from decomposition of the complex into simpler and more mobile defects. Excess defects may disappear from a crystal by two different mechanisms, migration to sinks and

recombination or annihilation.

Since there are quenched-in defects in the crystal, including free vacancies, one can expect that there should be a quenched-in excess conductivity, and that it would show an "enhanced conductivity" when the crystal is annealed. Dreyfus (5) and Layer et. al (15) have carried out isothermal annealing experiments in quenched crystals. Their results show that the annealing obeys first-order kinetics. However their experiments were carried out for relatively low quenching temperature. In metals, it has also been observed that the decay of excess-vacancies in isothermal annealing may follow first-order kinetics. But in the case of a higher quenching temperature, this annealing effect does not show first-order decay (20). Hence, whether or not the decay behavior would show first-order kinetics under the higher quench temperature seems uncertain.

EXPERIMENTAL PROCEDURES

A) Specimen Preparation

Pure LiF single crystals, designated as B3 and B5, had been obtained from the Harshaw Chemical Co., and were analyzed by the American Spectrographic Laboratories, who reported 1ppm and 3ppm mole fraction of Mg^{2+}, respectively, as the main impurity in these crystals. Doped crystals of LiF originally grown in Laboratories of Stanford University contained doping levels of 160ppm and 320ppm of Mg^{2+}, are designated H3 and H5, respectively. Crystals produced from powdered LiF obtained from American Fluoride Company and Baker and Adamson reagent grade material are denoted A and R respectively. The doping levels of all of the specimens are shown in table 2 as cation site fraction in parts per million. As determined, B5, A2 and A3 were confirmed to be doped with OH-ions (21).

Single crystal specimens 7 x 7 x 1mm thick were prepared by cleavage, and painted with a conducting coating of colloidal carbon on both the specimen surfaces to insure good electrical contact with the electrodes for conductivity measurements.

For quenching and annealing tests, specimens of different thickness were prepared by cleavage. One group

Table 2

Crystal-doping levels given as site fraction

crystal	doping-level (ppm)	remarks
B3	1 Mg	pure
B5	3 Mg	OH-doped
A2	5 Mg	"
A3	100 Mg	"
H3	160 Mg	
R2	190 Mg	
H5	320 Mg	

has dimensions of 7 x 7 x 1mm, which were essentially the same dimensions as those for conductivity measurements. The other group has dimensions of 3 x 7 x 1.5mm which are thicker than the former group. The latter group was used for critical resolved shear stress measurements after quenching.

B) Conductivity Measurements

A schematic diagram of the conductivity equipment is shown in figure 3. Two different electrical measuring set ups were used to obtain the data. A Wayne Kerr Universal Bridge was used for AC measurements, for temperature above about 200°C. This bridge is capable of measuring a conductance as low as 10^{-10}mho. The frequency of operation is 1592 c/sec. The DC measurements, which are required for the low temperature regions (9), (22) i.e., from room temperature to around 200°C, were carried out using a Cary 401 Vibrating Reed Electrometer. Voltages were supplied by a regulated DC power supply at potentials of 250V on the low conductivity range and IV on high conductivity ranges. It is capable of measuring a conductance as low as 10^{-17}mho. Conductivity measurements were made by heating at 1 - 2°C/min between room temperature and 600°C in a dry nitrogen gas atmosphere.

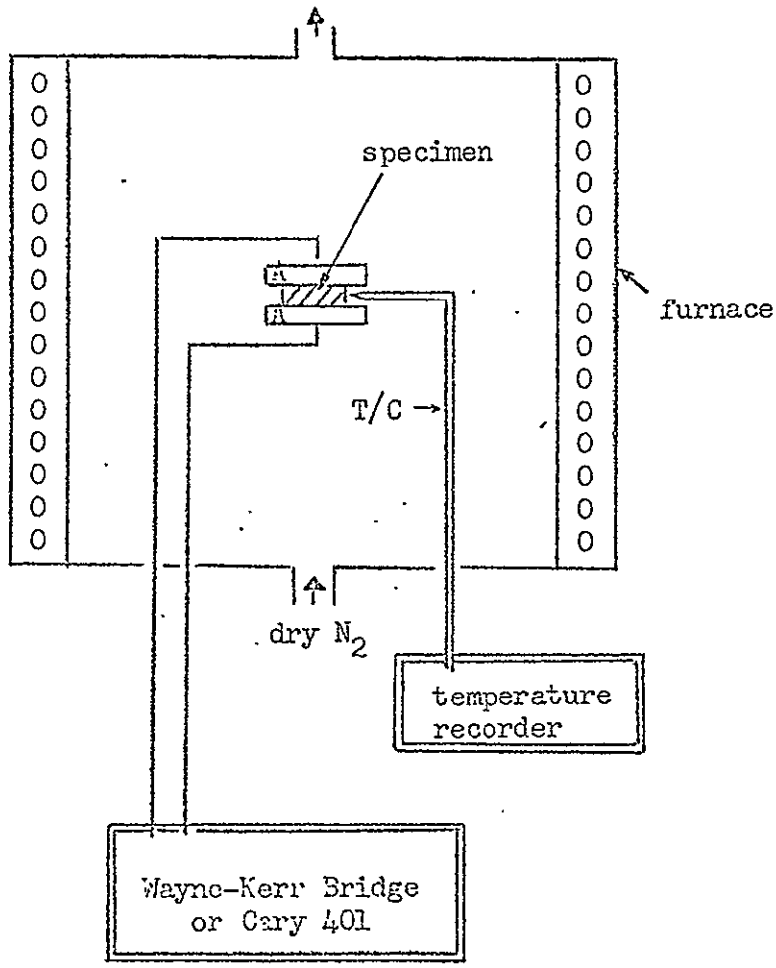

T/C : thermocouple
A : nickel electrodes

Figure 3. A schematic diagram of apparatus for conductivity measurements.

C) Quenching Method

Pure or doped crystals were quenched by using pre-cooled or dry He-gas, and an average quenching rate of 550°C/min was obtained. A schematic diagram of the quenching apparatus is shown in figure 4. The quenching rates were measured with a thermocouple inserted in a hole in a dummy specimen. After heating the specimen for an hour at the desired high temperature, the heating coil was dropped down away from the specimen and at the same time He gas (dry or pre-cooled) was blown into the furnace so that a rapid cooling of the LiF crystals was obtained. Several quenching curves are shown in figures 9 and 12. The quenching rate ranged from about 600°C/min for dry He gas to 1000°C/min for pre-cooled He gas in thin specimens. But in the case of the thick specimen, an average quenching rate of 550°C/min was obtained by using dry He gas. The quenching rate was taken as the average cooling rate from the quench remperature T_q to 50°C. After quenching from a temperature T_q of about 500°C or above, the specimens were coated with colloidal carbon and were placed in the conductivity furnace. In the case of the thick samples (thickness 1.5mm), one of the quenched specimens were used for critical resolved shear stress measurements.

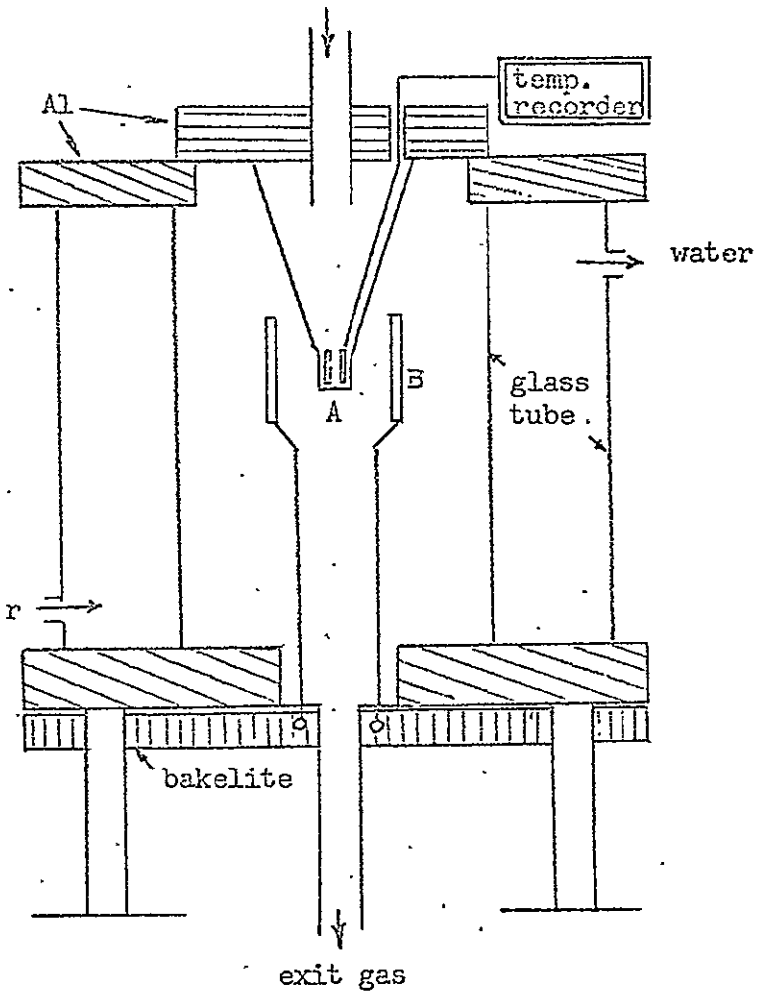

A: specimen and holder.
B: heating coil

Figure 4. A schematic figure of gas-quenching apparatus.

The decay of the conductivity during annealing was measured at various selected temperatures after keeping the quenched specimens at room temperaure for the 30 minutes which are required for preparation of the conductivity measurements. Annealing data are not available for this initial period. In addition, it took about 30 minutes to raise the temperature of the crystals from room temperature to the selected annealing temperature. Fluctuations about the selected annealing temperature were within $\pm 0.5^{o}C$, mostly within $\pm 0.25^{o}C$.

D) Measurement of the Critical Resolved Shear Stress

To examine whether quenching strains were induced, the critical resolved shear stress was measured. The compression axis was taken as the direction along the longest axis i.e., ⟨001⟩. The specimens were compressed at a strain rate of $2 \times 10^{-2} min^{-1}$ in a compression jig attached to an Instron testing machine, at room temperature (26).

RESULTS AND DISCUSSION

A) Ionic Conductivity

The overall picture of ionic conductivity followed the anticipated behaviour, discussed in the theory section. In figure 5, the results of conductivity plots are shown over 12 decades of σT. The intrinsic and free vacancy extrinsic region are clearly obtained for the specimen B3. At low temperature the regions are divided up to region VII, according to their slopes. In figure 5, the depressed conductivity plots for specimens A2 and A3 clearly show the existence of OH^--ion in these crystals (21).

(a) Intrinsic and extrinsic conduction (regions I and II)

In figure 6, which represents the high-temperature conductivity of the pure crystal, designated by B3, there is a definite increase in the slope of region I. This behaviour showing a continuous curve rather than a straight line is reported to be due to the contribution of anion vacancies (6), (9). Because of this curve in region I, it is not possible to assign an activation energy for the intrinsic conduction process, by only calculating the slope of region I in conductivity measurements. Rather, it is reasonable to use the results of Stoebe and Huggins

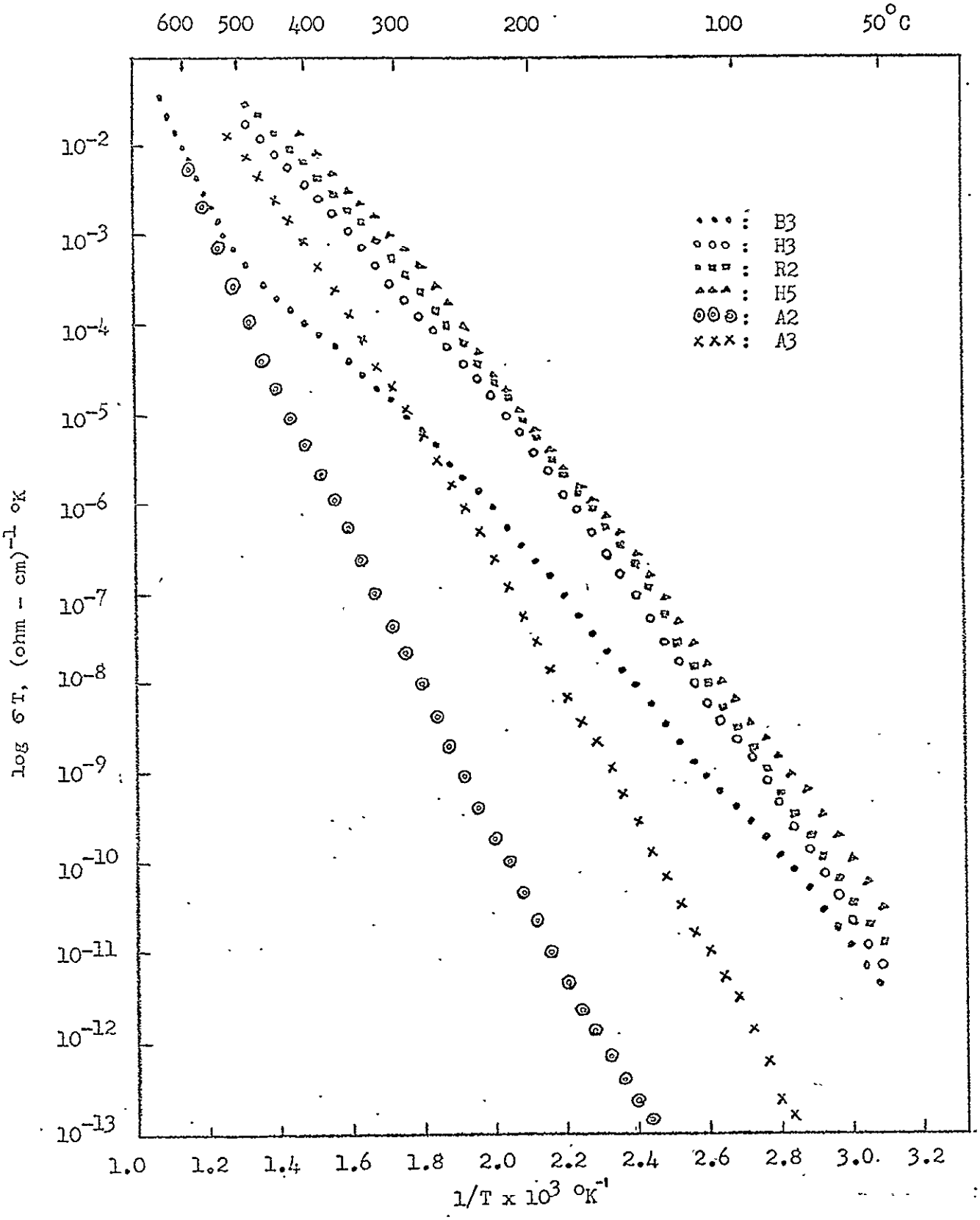

Figure 5. Ionic conductivity results.

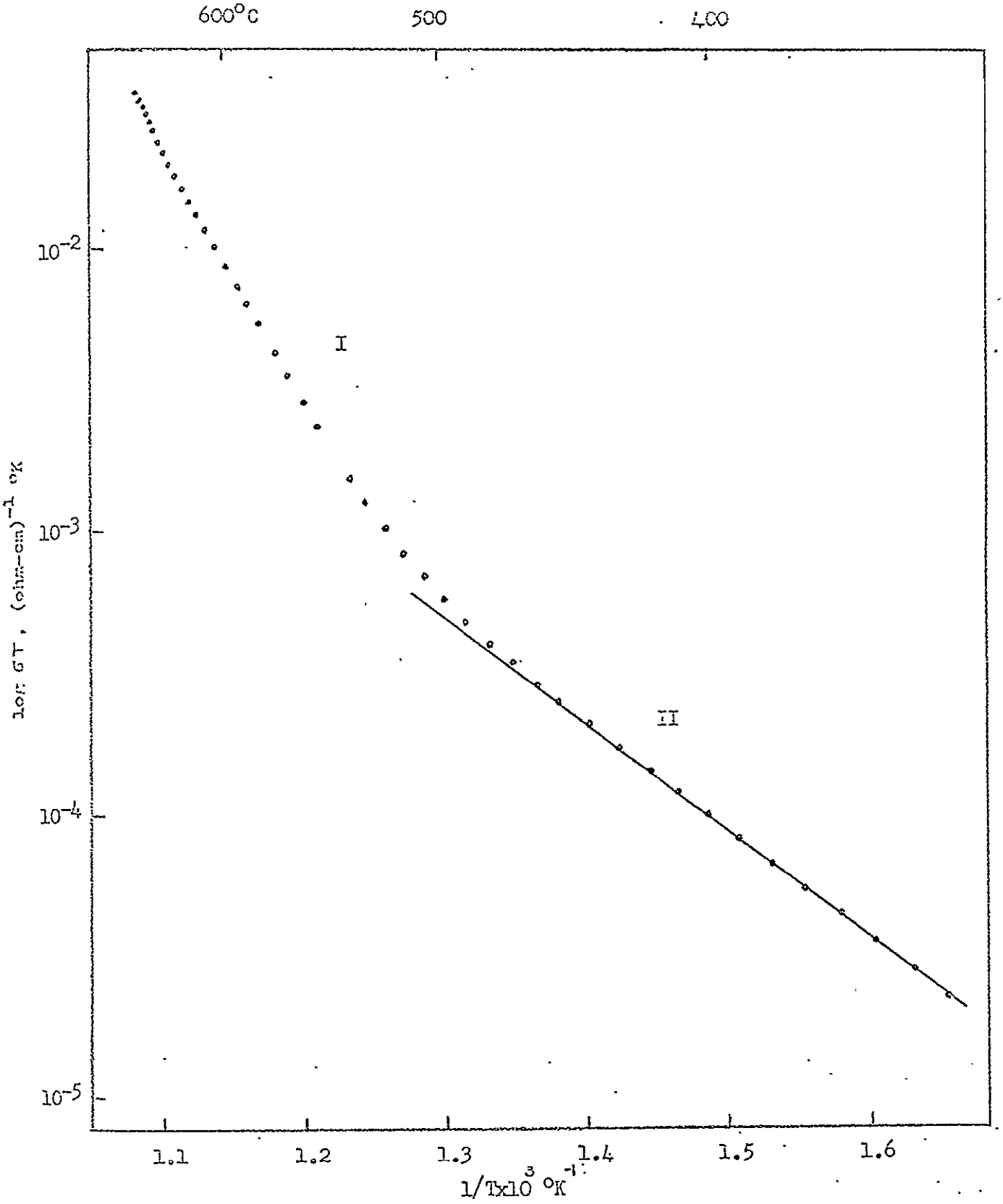

Figure 6. High temperature conductivity of pure crystal, B3.

who used diffusion data obtained by NMR measurements (27). Their results give 1.87eV the activation energy for the self-diffusion of lithium in LiF.

The conductivity results in region II, which is the free-vacancy extrinsic region, is also shown in figure 6. The slope of region II should yeild the energy of motion of cation vacancies according to equation (5). However, since region II extends over smaller ranges for increasing impurity concentrations, the inclusion of experimental points in the transition region above or below reion II tends to increase the slope of this region (28).

A straight line with the minimum slope in region II should give the best value for the motion energy of a cation vacancy (28). For the case of B3 a straight line can be drawn through the data points between 450°C and 340°C which gives an energy of motion of 0.73 $\pm$ 0.02eV. This value for E_m is slightly higher than the value of 0.70 $\pm$ 0.02eV obtained by Stoebe and Pratt (9), and the value of 0.70eV by Jain and Sootha (25), who worked with Ti-doped LiF. But it agrees well with the value of 0.73eV given by Barsis et.al (10) and the value of 0.72eV obtained by Eisenstadt (29).

Since the crystals of the present work and those of Stoebe and Pratt (9) were the same, it is a surprise

that there exists a discrepancy in activation energy. One of the reasons seems due to the state of equilibrium during conductivity measurements i.e., the fact that during the present work, the heating rate of 1 - 2°C/min was chosen instead of stepwise heating which gave steady-state conductivity data, and used in the work of Stoebe and Pratt. Therefore, it could be said that for the existence of discrepancies in the values of activation energy of region II given by several authors, there are two main reasons, one is the purity of crystal, and the other is state of euilibrium during measurements. Therefore, the best value for the motion energy of a cation vacancy is probably 0.72 $\pm$ 0.02eV.

Using this value of E_m = 0.72eV and the activation energy for region I of 1.87eV which has been mentioned above, the formation energy of a Schottky defect pair is found to be 2.30eV.

(b) Association region (region III) and lower temperature regions.

The conductivity curve at temperature below that of region II increases in slope gradually, usually as a continuous curve. Figure 7 shows region III for several crystals. The curves can be resolved into straight-line segments and the slopes of these segments yield the

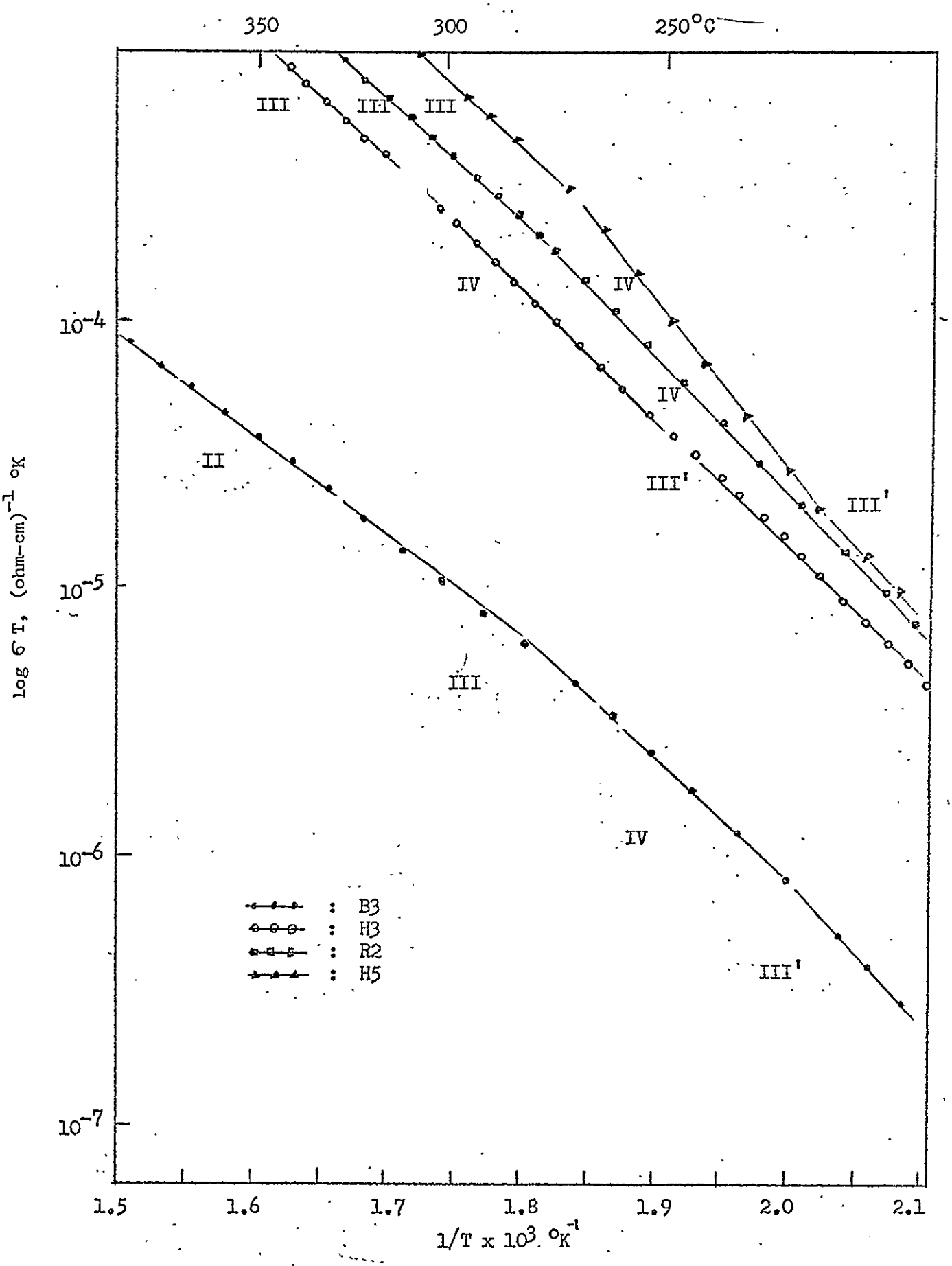

Figure 7. Intermediate temperature conductivity.

energies which have been given in table 3. Here it is shown that all crystals show a region III with an activation energy of about 0.90eV. From this slope, the association energy $E_A = 0.32 \pm 0.05$eV for Mg^{2+} in LiF is obtained. This value is somewhat lower than the value of 0.36eV given by Barsis et.al (10) and the value of 0.48eV obtained in Ti-doped LiF by Jain and Sootha (25). Below region III, it is at present difficult to assign a detailed mechanism for each region, because the theory as well as experimental evidence so far is insufficient. Figure 8 shows the conductivity plots which contains several regions.

Immediately below region III, the activation energy of about 1.00 ~ 1.05eV in general is obtained. The activation energy for this region IV seems to be due to the metastable precipitation of $MgF_2 \cdot 6LiF$ (5), (10). Below region IV, the slope of the conductivity plot usually decreases, which seems to be due to the freezing of precipitation mechanism and the continuation of dipole association. The values of this region, E_{III}' are almost the same as E_{III}.

The interpretation of the regions at lower temperatures is uncertain at present. The formation of trimers was reported for the lower temperature association

Table 3

Activation energy for each region(eV)

	B3	H3	R2	H5	remark	A2	A3
I	1.87*				intrinsic		
II	0.73		0.76	0.80	extrinsic	1.53	1.06
III	0.89	0.90	0.90	0.90	association	1.73	1.39
IV	1.05	1.00	1.03	1.29	$MgF_2$6LiF	1.43	1.23
III'	0.93	0.91		0.94	association	1.71	1.36
(V)	1.01	1.18	1.39	1.18	precipitates	1.26	1.62
(VI)	0.69	1.02	1.20	0.96			1.35
(VII)	1.07	1.28		1.37			1.52

* see text.

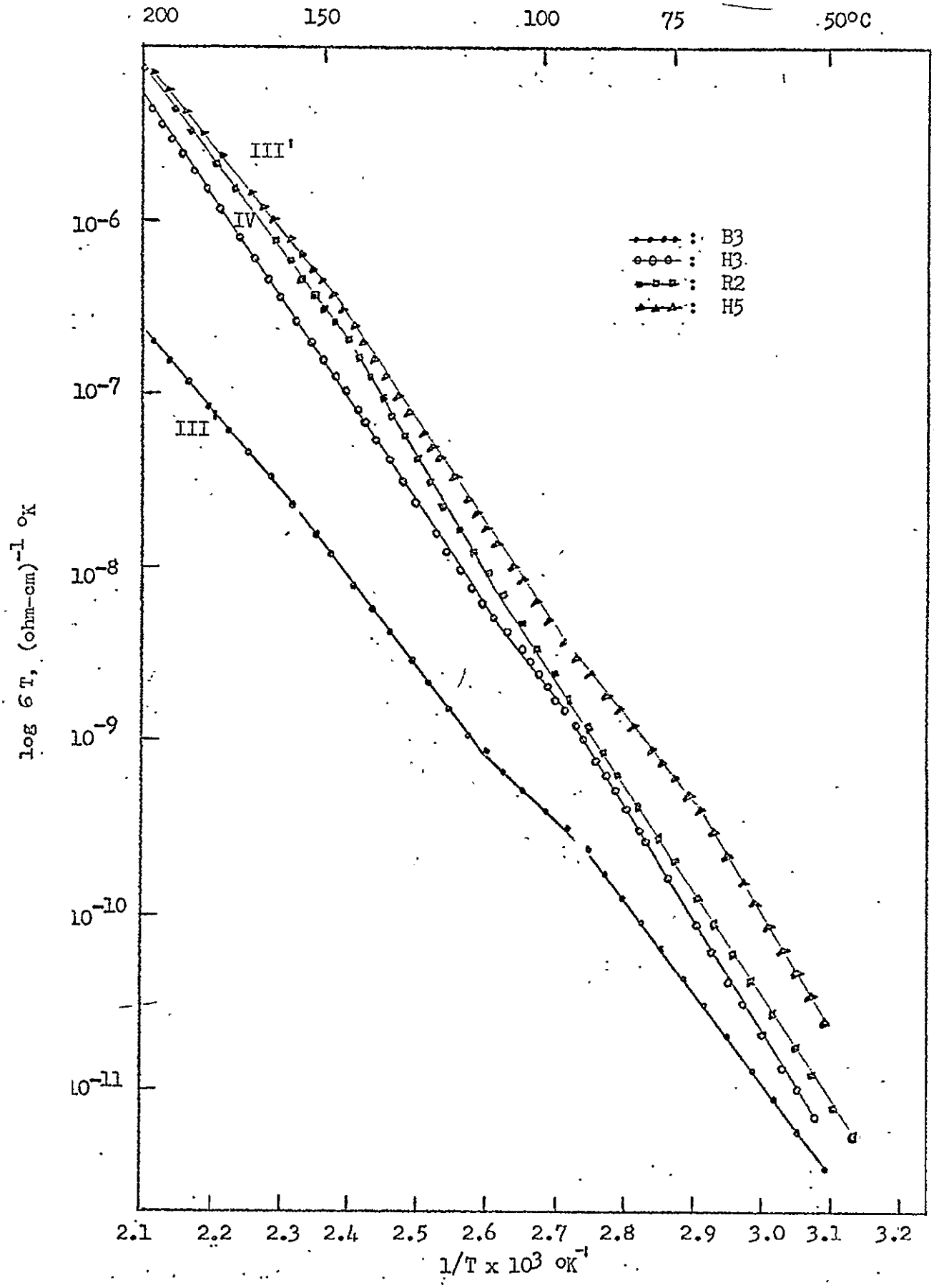

Figure 8. Low temperature conductivity.

(23), but this interpretation requires further study. In the room temperature region, the conductivity plots are almost parallel but are not coincident. Neither do the curves cross each other. It was also observed by Stoebe and Pratt (9) and is a difference from the work of Barsis et. al (10). This difference probably comes from the fact that their crystals were highly doped with Mg, compared to those of the present work.

(c) Effect of OH-ions

In figure 5 the conductivities of OH-doped crystals (A2 and A3) are shown. The activation energy of each region is shown in table 3. As shown in previous work (21), the conductivity of these crystals are greatly depressed. It is reported that the formation of various complexes such as the Mg-OH-vacancy complex decreases the effective amount of free vacancies which contribute to the ionic conductivity (21) (24).

B) Quenching and Annealing Effects

The annealing effect of the conductivity after quenching from high temperature (500°C-600°C) has been studied at several selected temperatures both on thin specimens and on thick specimens.

(a) Thin specimens (1mm)

In figure 9 several quenching curves are shown. The quenching rate ranged from about 600°C/min for dry He gas to 1000°C/min for pre-cooled He gas. After quenching the specimens were annealed at the selected temperatures. In figure 10 the decay behaviour of the quenched-in conductivity is shown for two annealing temperatures 83°C and 132°C. The origin of time was the time at which the temperature of the crystal reached the selected annealing temperature. The normalized decay behaviour, as shown in figure 11, confirms the first-order kinetics (5) (16), which suggests the presence of a time-independent number of trapping centers for the excess cation vacancies, and rules out the possibility that the predominant process is the recombination of vacancies with isolated impurities, since this process does not involve first-order kinetics.

During the quenching of thin specimens, the possibility of quenching strains was not considered, and since the specimens are thin and the decay behaviour in figure 11 is similar to those of Ninomiya (16) and Dreyfus and Nowick (5), it seems that quenching strains were not appreciable.

Since the magnitude of the enhanced conductivity was very small, it was difficult to analyze it conclusively.

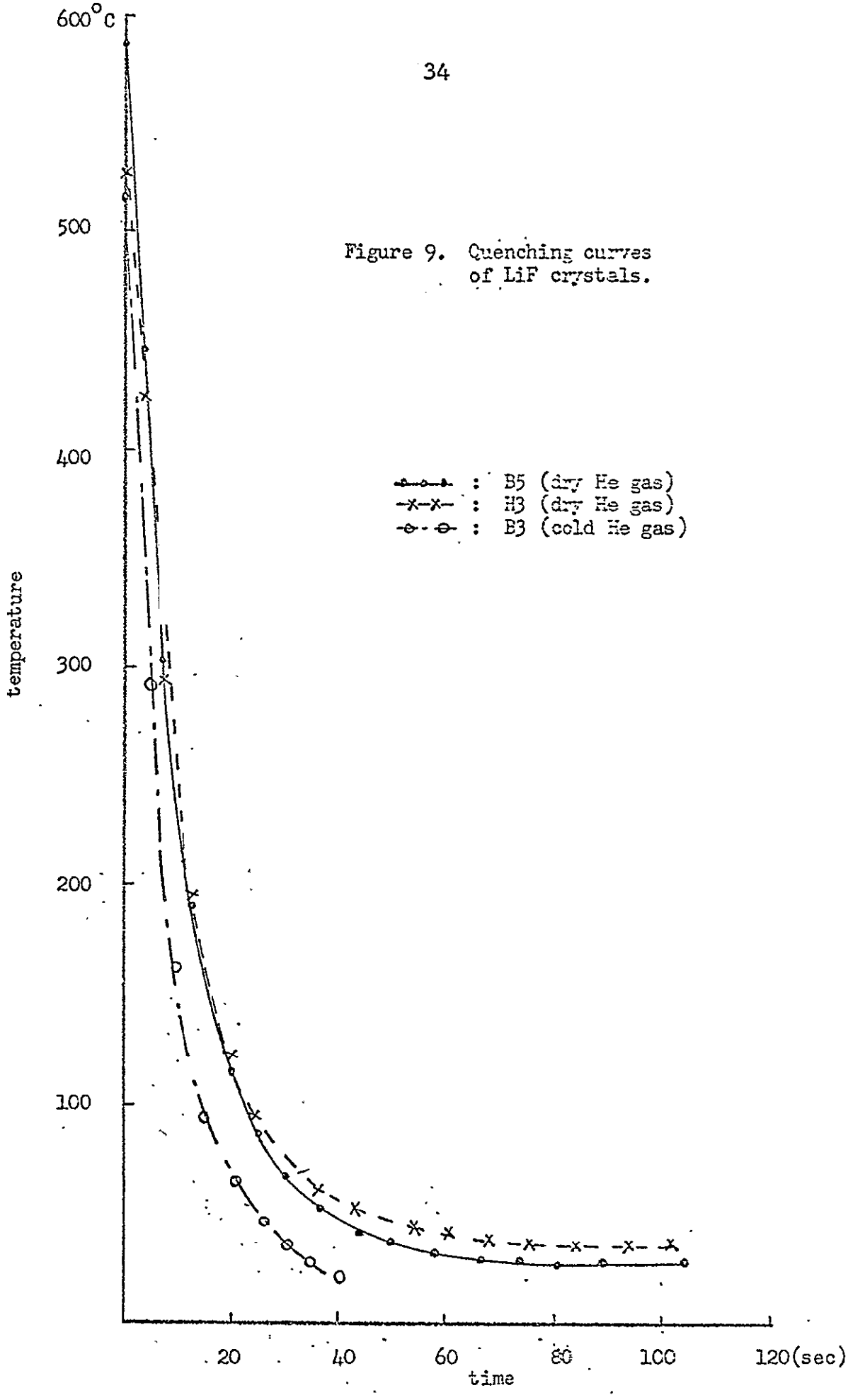

Figure 9. Quenching curves of LiF crystals.

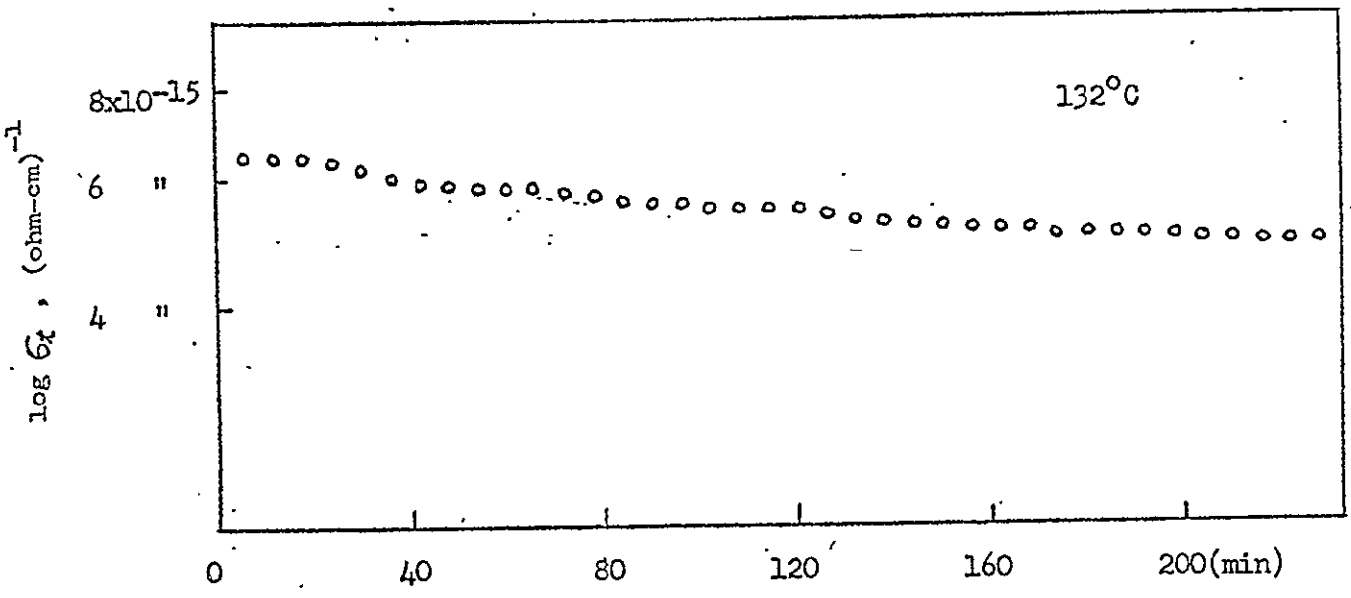

(a) B5, (T_q = 587°C)

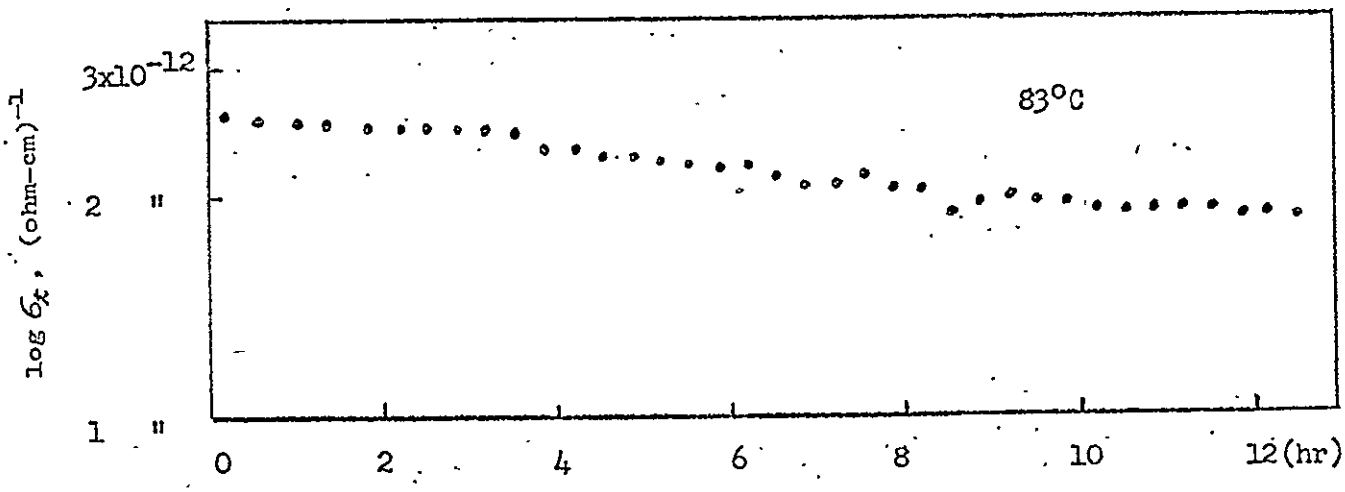

(b) H3, (T_q = 530°C)

Figure 10. The decay behavior of enhanced conductivity due to quenching.

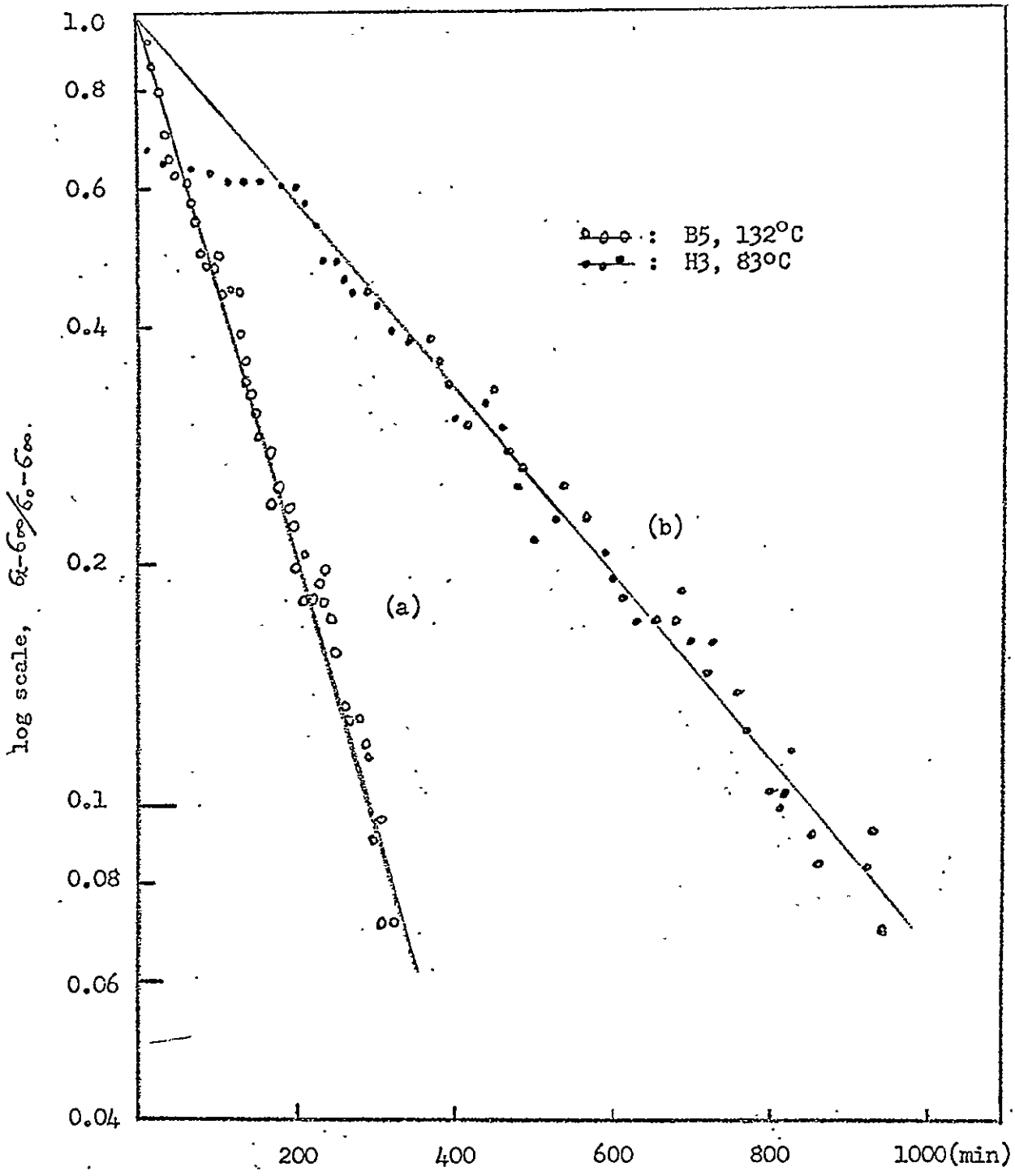

Figure 11. Normalized annealing curves of figure 10, showing that the kinetics are first order.

Because of this and the sensivity of σ to temperature fluctuation, it was not possible to find an activation energy of decay behavior by doing a series of annealing experiments for each doping level.

(b) Thick specimens (1.5mm)

In the hope to quench-in appreciable amount of free cation vacancies, thick specimens of pure crystal B3, which have dimensions 3 x 7 x 1.5mm, were chosen for the following experiment. For these specimens, 500°C was taken as quench temperature T_q, which is almost the knee temperature between region I and region II. Dry He gas was used as quench media for all these specimens. A typical quenching curve is shown in figure 12, in which quenching rate is 550°C/min. All the quenching rates for these specimens were about 550°C/min.

The decay behavior of the quenched-in conductivity during annealing shows an anomaly in contrast to those of the thin specimens. A peak in conductivity vs. time curve was found during the initial period of annealing except for the case of a room temperature annealing. In figures 14 through 16, the anomalous behavior of the quenched-in conductivity, σ_x, is shown with the temperature of the specimen in lower part. Here, the origin of time was the

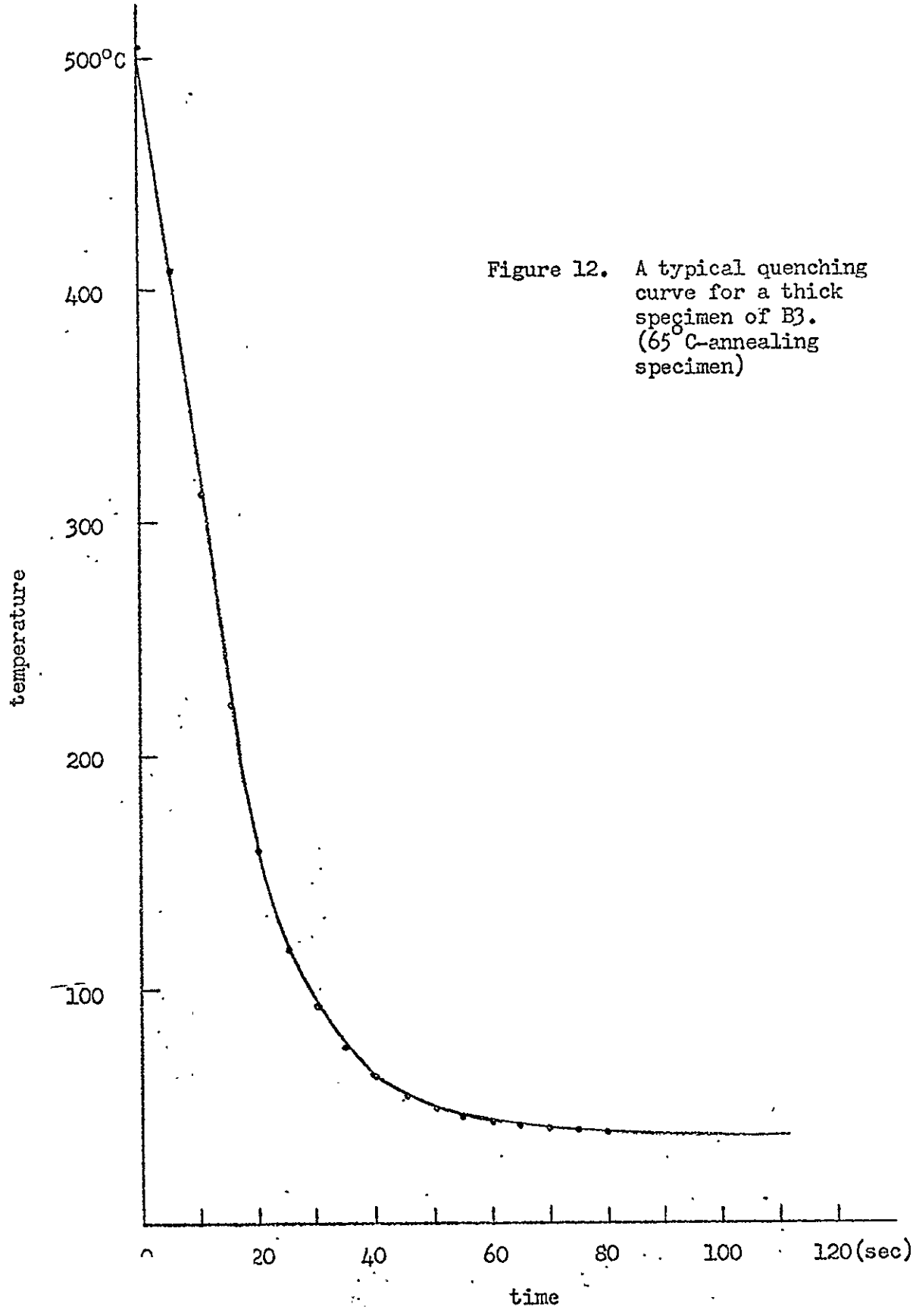

Figure 12. A typical quenching curve for a thick specimen of B3. (65°C-annealing specimen)

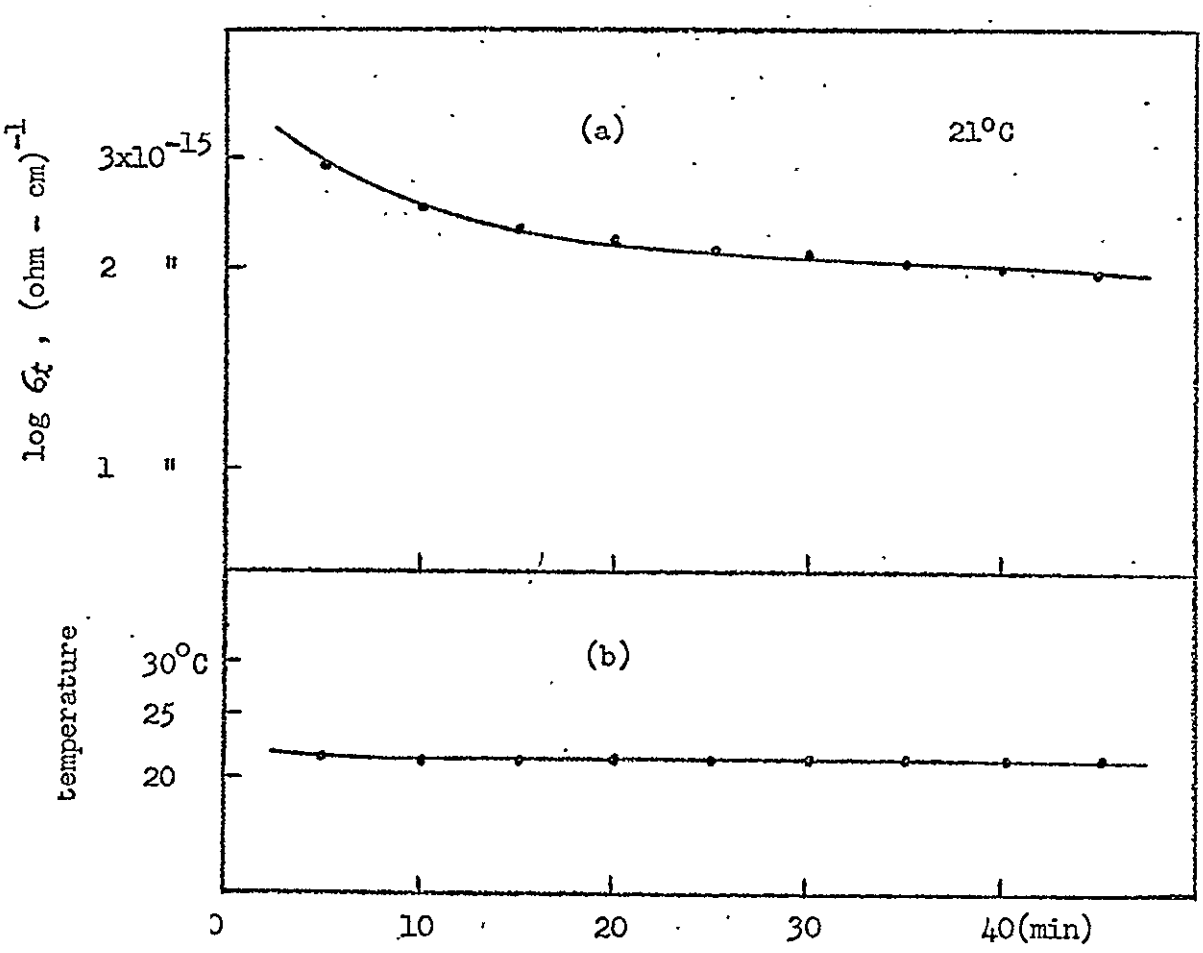

Figure 13. (a) Isothermal conductivity σ_t vs. time during room temperature annealing(21°C).

(b) The temperature of specimen during annealing.

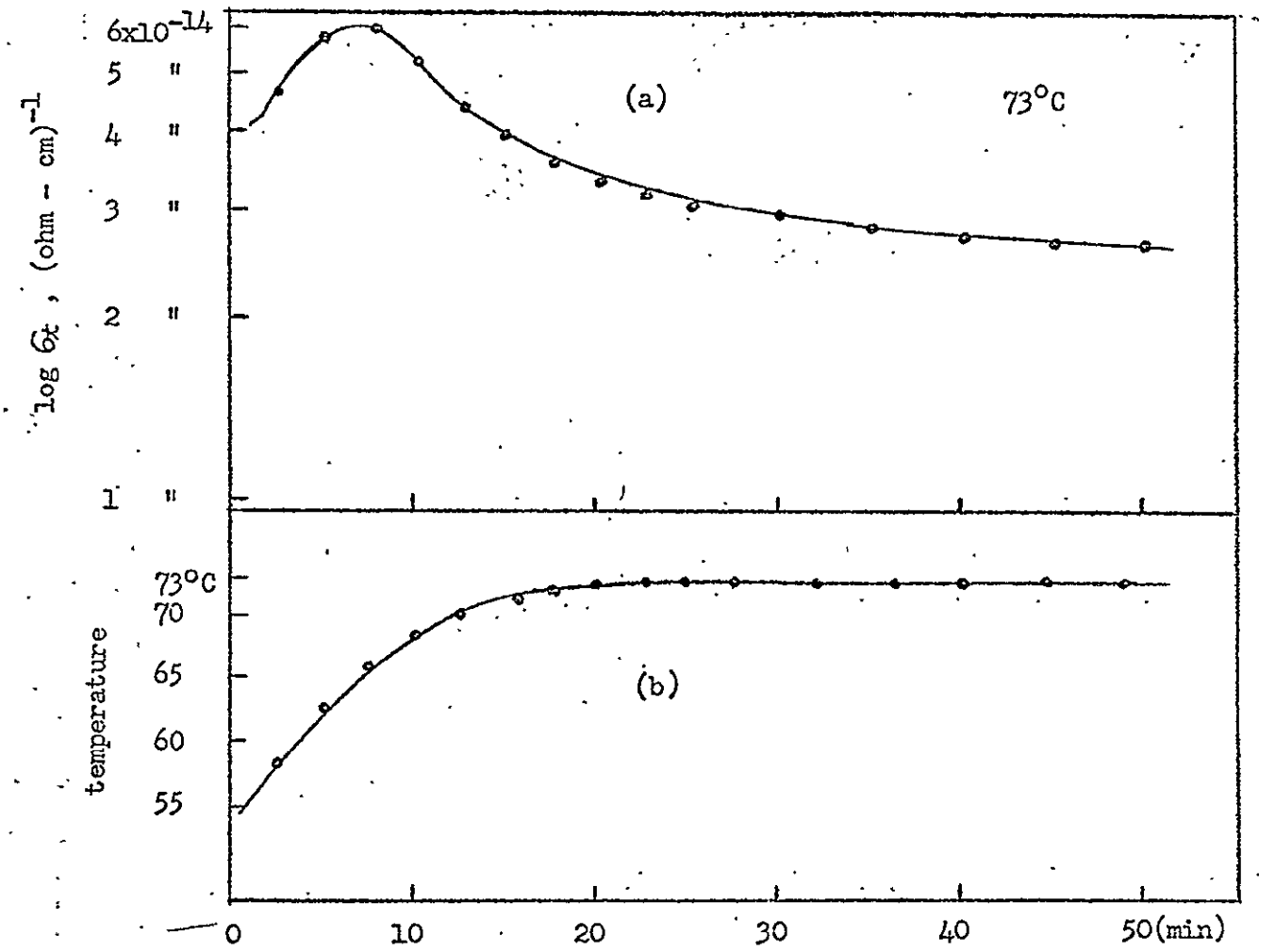

Figure 14. (a) Isothermal conductivity σ_t vs. time during 73°C-annealing.

(b) The temperature of specimen during annealing

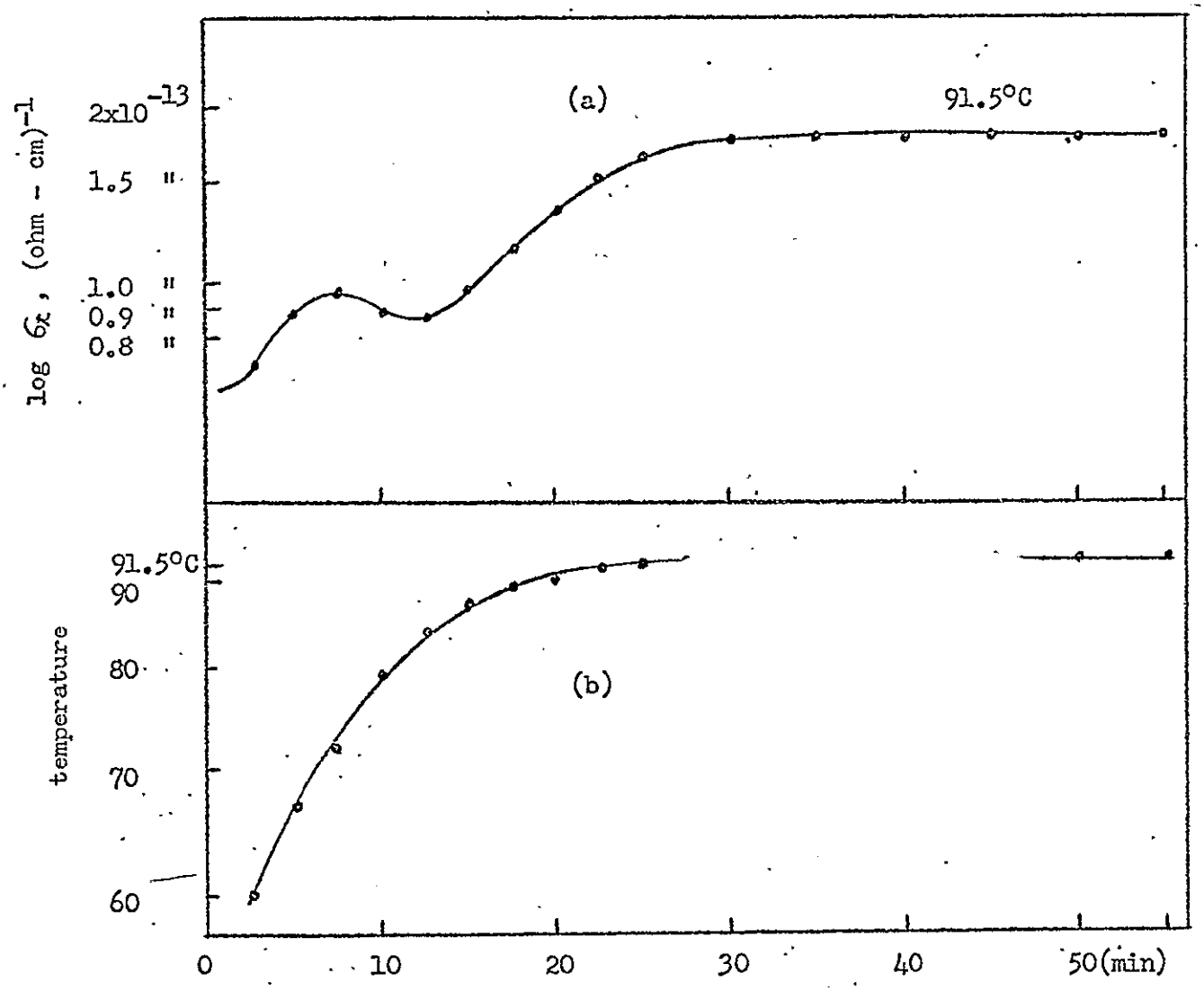

Figure 15. (a) Isothermal conductivity σ_t vs. time during 91.5°C-annealing.

(b) The temperature of specimen during annealing.

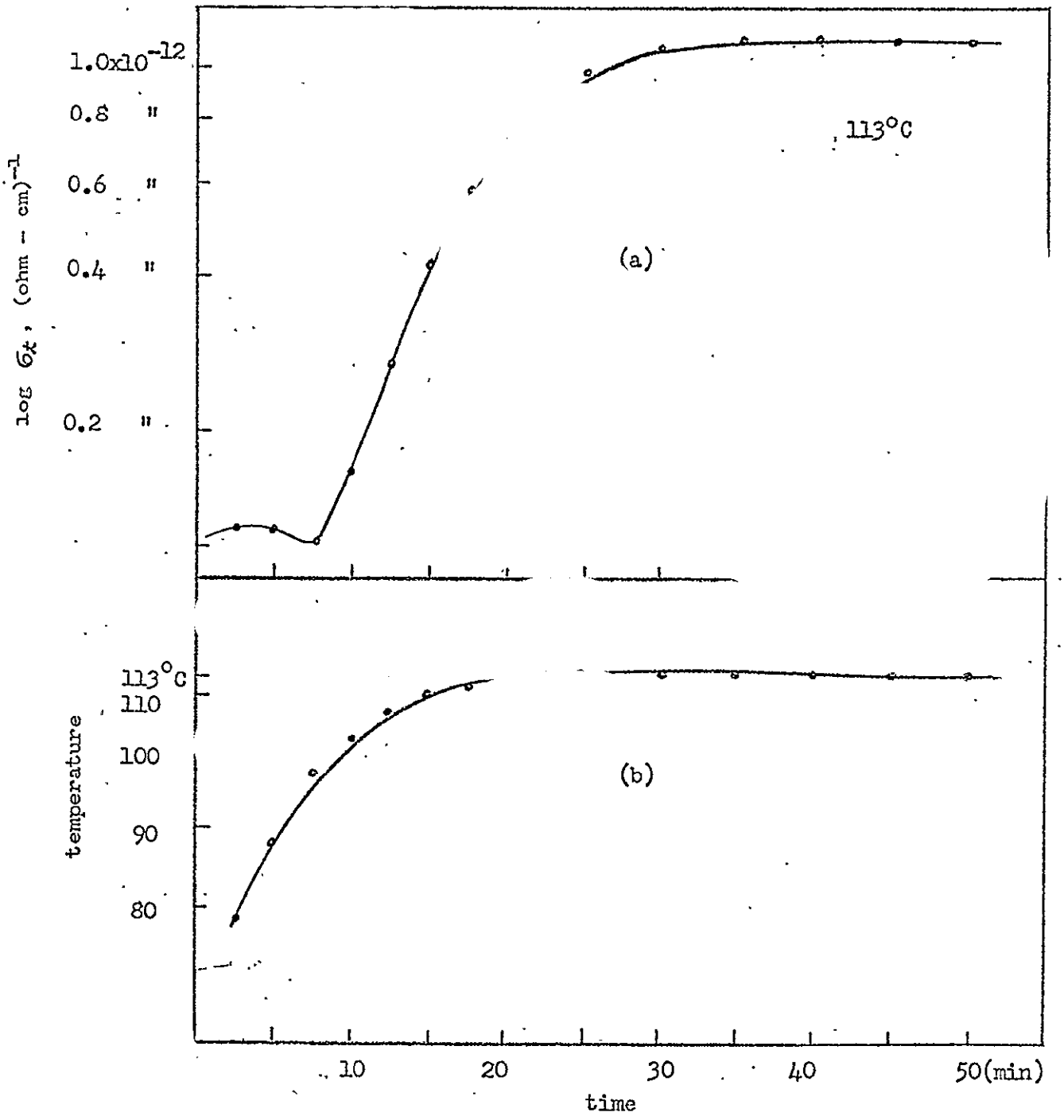

igure 16. (a) Isothermal conductivity σ_t vs. time during 113°C-annealing.

(b) The temperature of specimen during annealing.

time at which the electric field was applied, which was immediately after the specimen was placed in the conductivity furnace. The results for the annealing temperatures 56°C and 65°C was similar to the figure for annealing temperature 73°C. As shown in figures 14 through 16, a peak in conductivity appears before the actual temperature of the specimen reaches the equilibrium temperature and decays first rapidly and then slowly. In case of high temperature annealing such as 91.5°C and 113°C, the decay following a peak was soon marked because the equilibrium temperature itself was very high.

For better clarity, in figure 17, conductivity σ_x was plotted with time such that all the peaks for each annealing temperature except for room temperature be coincident. In figure 18 the values of $\sigma_x - \sigma_{normal}$, where σ_{normal} is the value of σ at each corresponding temperature in an off-quench crystal, are plotted as a function of time. The width of the peaks decreases with increase in temperature, which suggests that the mechanism for the anomaly becomes more active with increasing in temperature. In figure 19 normalized conductivities in the slowly-decaying part of figure 17 were plotted as a fuction of time. Therefore the origin of time is the time at which the slow decay was fully set up. From this decay

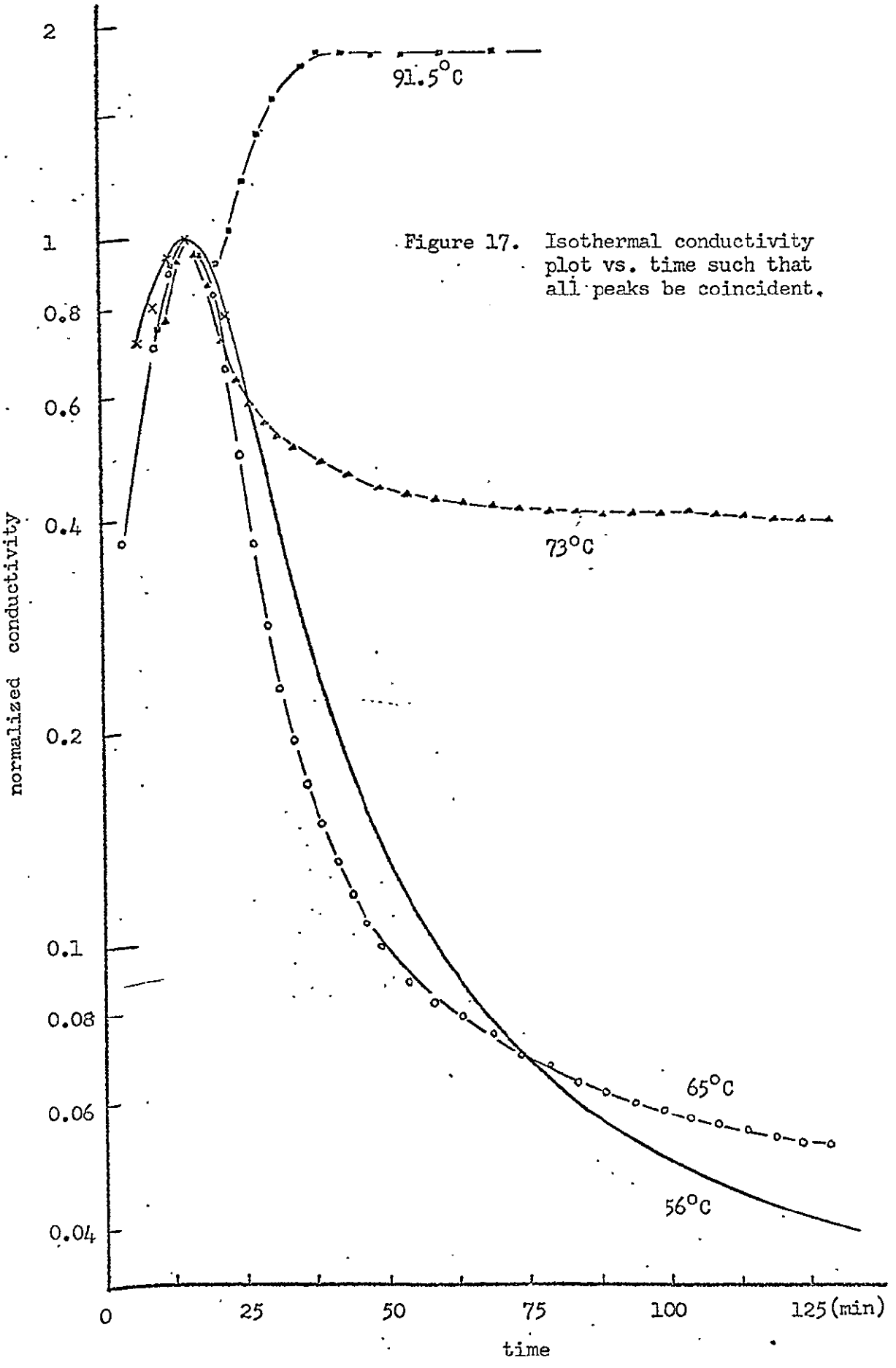

Figure 17. Isothermal conductivity plot vs. time such that all peaks be coincident.

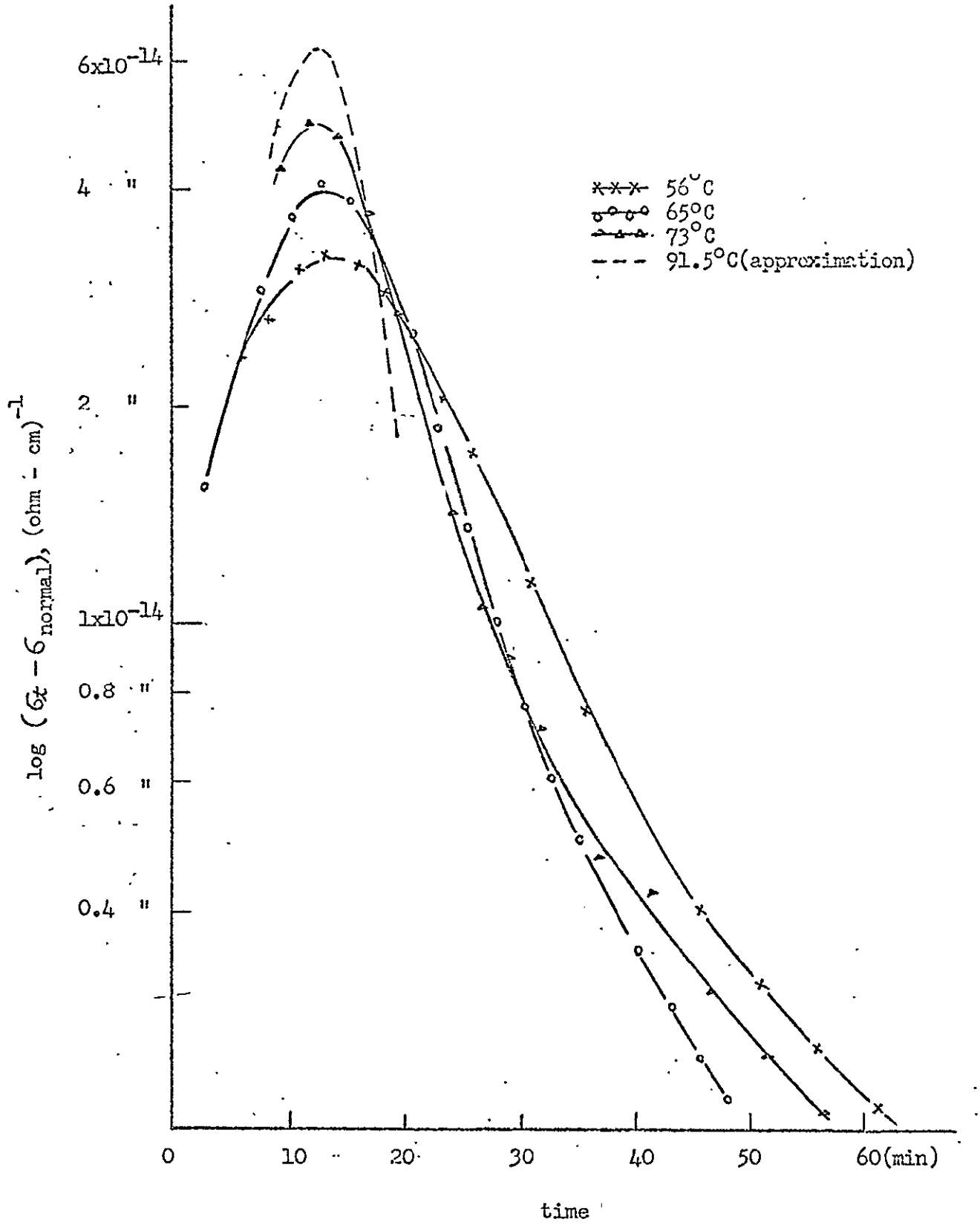

Figure 18. $\sigma_t - \sigma_{normal}$ vs. time. It shows the peak height and the width of peak at each annealing temperature.

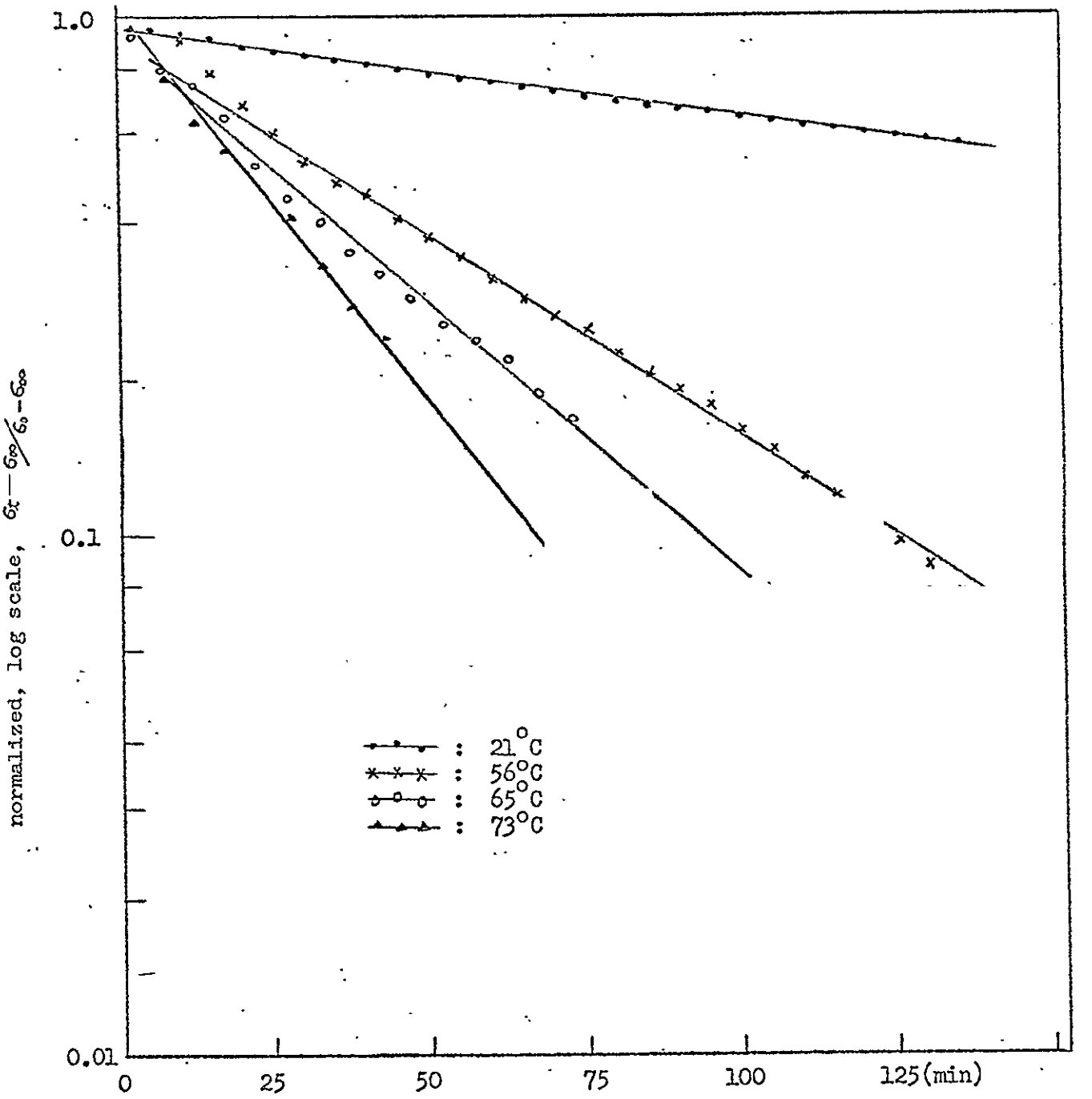

Figure 19. Normalized conductivity in slow-decay part of figure 17.

behavior, the activation energy of 0.33 ± 0.1eV was determined as shown in figure 20.

(c) Effect of quenching strains in the thick specimens.

An increase in the ionic conductivity during the annealing of a quenched specimen of an ionic crystal was not reported so far, except in the work of Petiau (23) on LiF. In the work, a peak was observed in the conductivity, σ_x, during annealing at 95°C following rapid quenching from 300°C. It was suggested that the dissociation of impurity-vacancy dipoles during the initial period of the annealing increases the effective concentration of free cation vacancies. However, the possibility of influence of quenching strains on conductivity was not mentioned and thus the dissociation of impurity-vacancy dipole could not be understood. At the same time, Petiau (23) demonstrates that a continuous decreases in the impurity-vacancy dipole concentration occurs by measuring the dielectric loss peak as a function of time. From the work of Cook and Dryden (13) it was shown that the decrease in the vacancy-impurity dipole concentration of quenched crystal is due to the formation of trimers during isothermal annealing. Then during annealing at higher temperatures, some of impurity-vacancy dipole should break

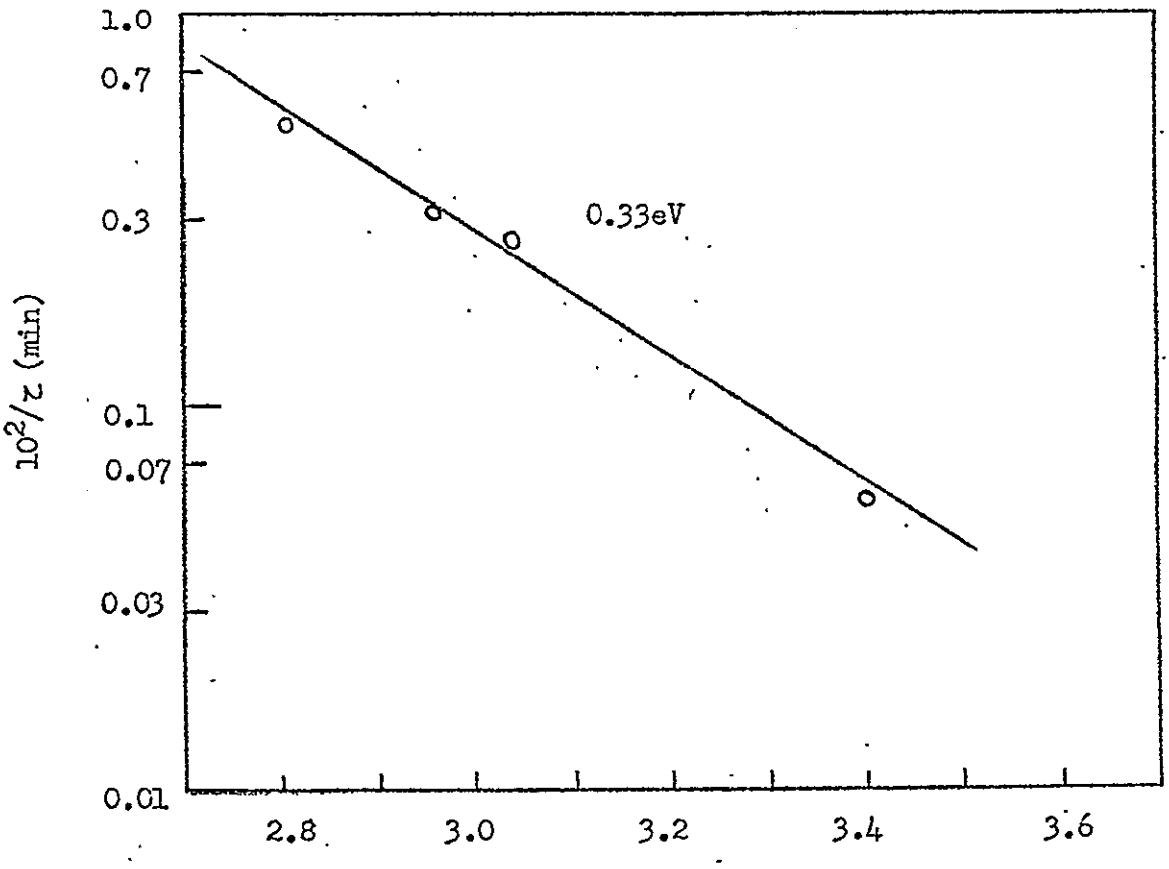

Figure 20. The reciprocal of relaxation time (τ) for decay of excess conductivities in figure 19.

up into isolated impurities and free cation vacancies, while some of the dipoles aggregate to form trimers. But this mechanism seems unrealistic because the temperature is not high enough that thermal energy itself could dissociate the impurity-vacancy dipole. Rather, the already existing dipoles should further aggregate continuously to form trimers.

To detect whether or not quenching strains were introduced by quenching, the critical resolved shear stress was determined after quenching, and is shown in figure 21. The shear stress increased slightly in quenched specimen with quench temperature T_q above 300°C. This increase in the shear stress corresponds approximately to the flow stress of 1% deformed crystal. Thus it seemed possible to connect the peak in conductivity during annealing with any effect of dislocations which was created during quenching.

In figure 22 two isothermal conductivity curves are shown; one is the annealing curve of the quenched specimen at 65°C and the other one is that of a crystal deformed 1% in compression at room temperature and annealed at 62°C. A very similar behavior of these two crystals was observed during annealing, which implies the presence of a dislocation effect on conductivity.

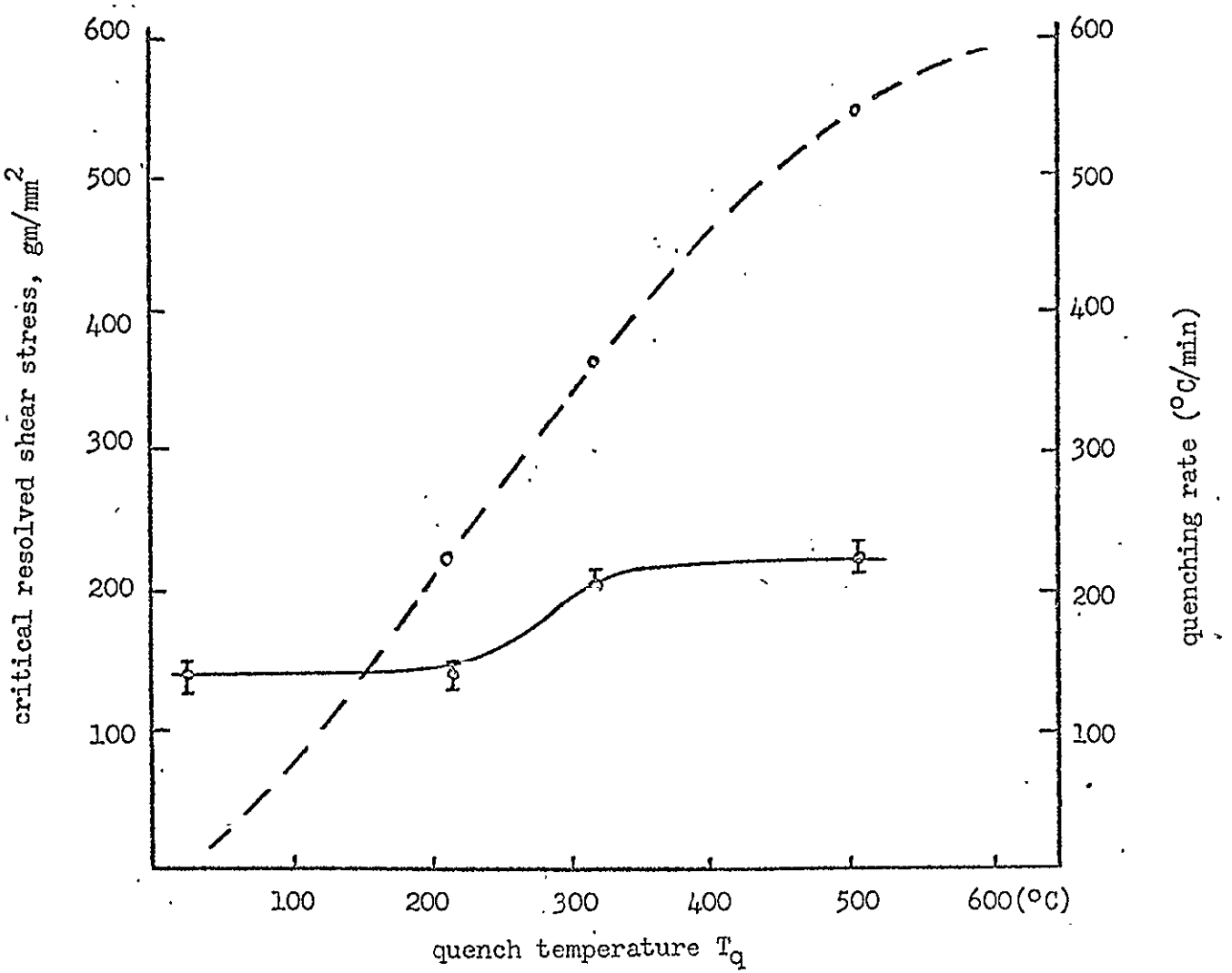

Figure 21. Room temperature critical resolved shear stress of quenched B3 vs. quench temperature T_q. The quenching rate at each T_q is shown as dotted line.

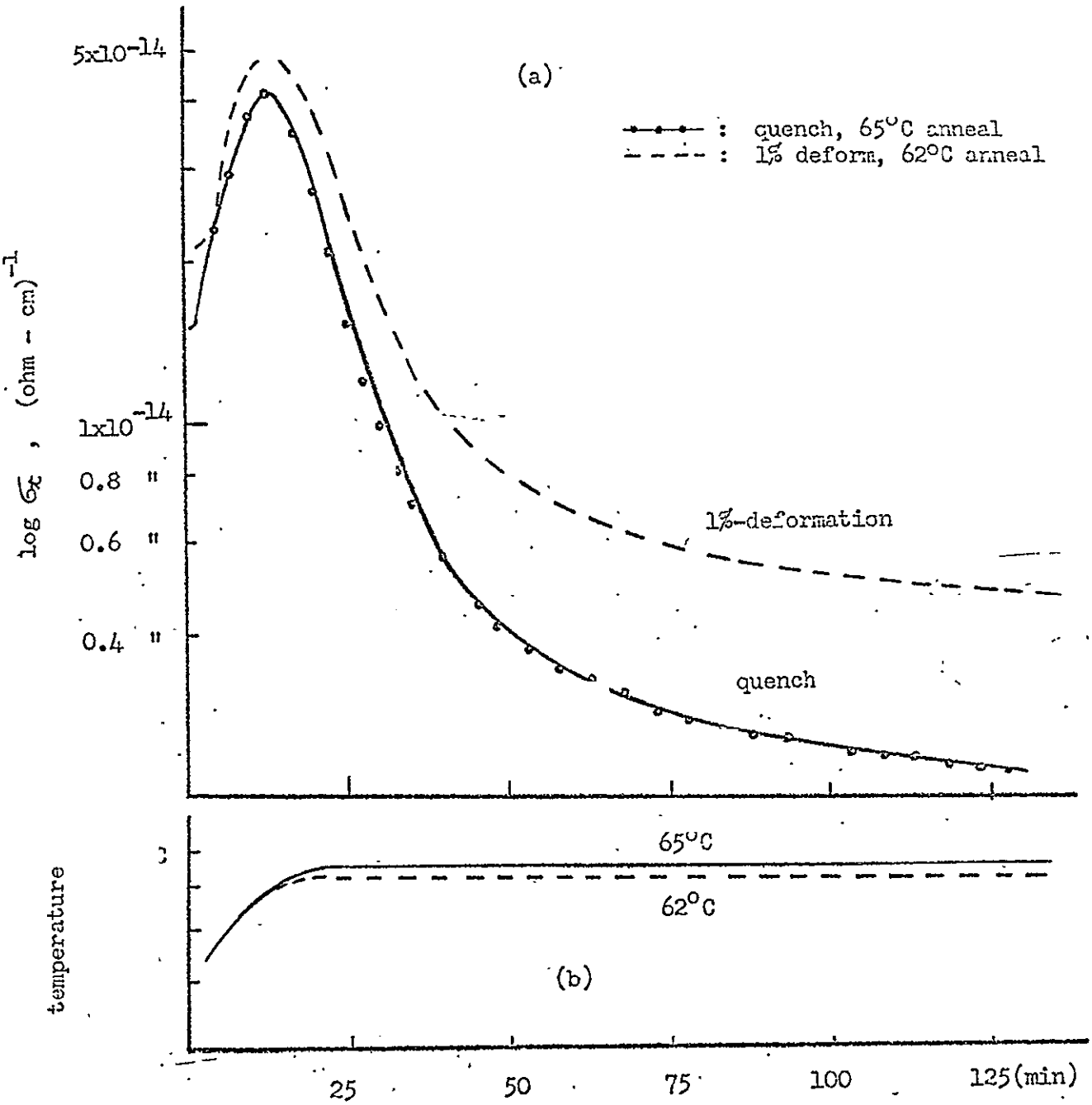

Figure 22.

(a) *Comparison of annealing effect on conductivity.* Solid line for the specimen annealed at 65°C, after 500°C-dry He gas quench. Dotted line for the specimen annealed at 62°C, after 1% room temperature deformation.

(b) The temperature of specimen during annealing.

Therefore, it is considered that excess free cation vacancies, which are bound to moving dislocations during rapid quenching or deformation are released from the dislocations and thus give rise to an increase in the conductivity. During quenching, the free cation vacancies, which are negatively charged, become bound to jogs on moving dislocations. When the crystal is heated slightly during annealing after quenching, these excess free cation vacancies are released from the dislocations and migrate through the lattice, causing increased conduction. Subsequently these excess vacancies anneal out at sinks or form dipoles with isolated divalent impurities. In case of room temperature annealing, the low temperature can not assist the releasing of cation free vacancies. The interpretation of the low activation energy 0.33eV is still uncertain, but it may be connected with the binding energy between the excess free cation vacancies and the dislocations.

SUMMARY AND CONCLUSIONS

(1) In the high temperature part of region I, (intrinsic region), the anion vacancy contribution to ionic conductivity in LiF was confirmed.

(2) The formation energy of a Schottky pair is 2.30eV, while the activation energy for cation vacancy motion, E_m, is 0.72 ± 0.02eV.

(3) The decay behavior of excess quenched-in vacancies in thin specimens was found to follow first-order kinetics during annealing.

(4) The decay behavior of excess vacancies in thick specimens showed an anomalous increase in conductivity during the initial period of annealing, which could be due to the release of free vacancies which are bound to dislocations during quenching.

REFERENCES

(1) A. B. Lidiard, Handbuch der Physik, edited by S. Flugge (Springer-Verlag, Berlin, 1957), Vol. 20, P.246.

(2) P. Suptitz and J. Teltow, Phys. Stat. Sol., 23, 9 (1967).

(3) W. Lehfeldt, Z. Physik, 85, 717 (1933).

(4) E. Koch, and C. Wagner, Z. Physik Chem. Abt., B38, 295, (1937).

(5) R. W. Dreyfus and A. S. Nowick, Phys. Rev., 126, 1367, (1962).

(6) D. L. Kirk and P. L. Pratt, Proc. Brit. Ceram. Soc., 9, 215 (1967).

(7) Y.Haven, Rec. Trav. Chem. Pays-Bas., 69, 1471(1950).

(8) Y. Haven, ReC. Trav. Chem. Pays-bas., 69, 1505 (1950).

(9) T. G. Stoebe and P. L. Pratt, Proc. Brit, Ceram. Soc., 9, 181, (1967).

(10) E. Barsis, E. Lilley, and A. Taylor, Proc. Brit. Ceram. Soc., 9, 202 (1967).

(11) A. B. Lidiard, J. Appl. Phys., 33, 414 (1962).

(12) R. W. Dreyfus and A. S. Nowick, J. Appl. Phys. 33, 473 (1962).

(13) J. S. Cook and J. S. Dryden, Proc. Phys. Soc., 479, 80 (1962).

(14) J. S. Dryden and R. J. Meakins, Disc. Faraday Soc., 23, 29 (1957).

(15) H. Layer, M. G. Miller and L. Slifkin, J. Appl. Phys., 33, 478 (1962).

(16) T. Ninomiya, J. Phys. Soc., Japan, 15, 1601 (1960).

(17) J. Quin, B. A. W. Redfern and P. L. Pratt, Proc. Brit. Ceram. Soc., 9, 35 (1967).

(18) J. S. Cook and J. S. Dryden, Aust. J. Phys., 13, 260 (1960).

(19) W. G. Johnston, J. Appl. Phys., 33, 2050 (1962).

(20) J. E. Bauerle and J. S. Koehler, Phys. Rev., 107, 1493 (1957).

(21) T. G. Stoebe, J. Phys. Chem. Solids, 28, 1375 (1967).

(22) P. H. Sutter and A. S. Nowick, J. Appl. Phys., 34, 734 (1963).

(23) J. Petiau, J. de Phys., 24, 564, (1963).

(24) A. Kessler and E. Mariani, Czech, J. Phys. B17, 786 (1967).

(25) S. C. Jain and G. D. Sootha, Technical Report No. 1, Project No. NBS (G)-32 (Under PL 460 Program), Indian National Physical Laboratory (1965).

(26) M. Srinivasan, M. S. Thesis, University of Washington, (1969).

(27) T. G. Stoebe and R. A. Huggins, J. Mtls Sci., 1, 117 (1966).

(28) S. C. Jain and S. L. Dahake, Indian J. Pure Appl Phys., 2, 71 (1964).

(29) M. Eisenstadt, Phys. Rev., 133, A191 (1964).